overlap against the previously reported repertoire of putatively-functional long non-coding RNAs (Guttman et al. 2009). We considered that these intergenic TSCs were not derived from our experimental errors, especially those identified in DLD-1 cells (Barski et al. 2007; Welboren et al. 2009), since we detected clear binding signals for pol II around 61 (21%) and 2 (2%) intergenic TSC targets of HIF-1α. These results collectively suggested that we had identified putative non-protein-coding transcript targets of HIF-1α that were comparable to the canonical RefSeq targets with respect to the number of targets and their levels of induction. However, further analyses are needed to determine the biological relevance underlying the induction of these non-coding transcripts.

Conclusion

In the present paper, we describe the genome-wide identification of HIF-1α binding sites in the cancerous DLD-1 cell line and the normal lung fibroblast TIG-3 cell line using ChIP-Seq. We utilized several types of Illumina GA analyses to further characterize the identified binding sites. The greatest advantages of using massively parallel sequencers may be the ability to obtain versatile biological data. In fact, we were able to obtain extensive biological information that allowed us to interpret the binding events; such information could not have been obtained using ChIP-chip or microarray analysis alone. We unexpectedly discovered that HIF-1α binding sites regulate an unexpectedly large population of alternative promoters and putative non-coding transcripts. These categories of the transcripts may also contribute to hypoxic response of the cell, though they have been overlooked in previous studies. The analyses targeting these transcripts were first enabled by the single-base resolution of massively parallel sequencing technologies, for which no previous knowledge was necessary for the probe design.

An obvious limitation of the present study was the use of only two cell types. Thus, we could not identify all of the possible binding sites of HIF-1α. The identification of different targets in DLD-1 and TIG-3 cells indicates that similar analyses should be conducted using a wider variety of cell types. In addition, our stringent criteria may have precluded the identification of many genuine targets. Indeed, some genes that have been well characterized as HIF-1α target genes were not found in our study, including the telomerase (TERT) gene (Nishi et al. 2004), the vascular endothelial growth factor A (VEGFA) gene (Carmeliet et al. 1998; Forsythe et al. 1996) and the erythropoietin gene (Semenza and Wang 1992) [also note that this result is similar to that obtained in a previous ChIP-chip analysis (Mole et al. 2009)].

All of the data generated in the present study were essentially the sequence data; however, we believe that the applications of massive sequencing at various biological levels have yielded substantial biological indications. We could find that the epigenetic regulation of chromatin status and the differential repertoires of expressed transcription factors played essential roles in the cell-type-specific induction of target genes in DLD-1 and TIG-3 cells in response to hypoxia. Further extensive analyses of epigenetic changes in cancer and normal cells using Nucleosome-Seq and ChIP-Seq and of the expression patterns of transcriptions factors using TSS-Seq or RNA-Seq could reveal the mechanisms by which the differential responses of various cells to hypoxia are encoded. Such information could reveal how hypoxic cellular responses are mediated by HIF-1α in a wide variety of cancer cells.

References

Albert I, Mavrich TN, Tomsho LP, Qi J, Zanton SJ, Schuster SC, Pugh BF (2007) Translational and rotational settings of H2A.Z nucleosomes across the *Saccharomyces cerevisiae* genome. Nature 446:572–576

Ashburner M, Ball CA, Blake JA, Botstein D, Butler H, Cherry JM, Davis AP, Dolinski K, Dwight SS, Eppig JT, Harris MA, Hill DP, Issel-Tarver L, Kasarskis A, Lewis S, Matese JC, Richardson JE, Ringwald M, Rubin GM, Sherlock G (2000) Gene ontology: tool for the unification of biology. The gene ontology consortium. Nat Genet 25(1):25

Barski A, Cuddapah S, Cui K, Roh TY, Schones DE, Wang Z, Wei G, Chepelev I, Zhao K (2007) High-resolution profiling of histone methylations in the human genome. Cell 129(4):823–837

Benita Y, Kikuchi H, Smith AD, Zhang MQ, Chung DC, Xavier RJ (2009) An integrative genomics approach identifies hypoxia inducible Factor-1 (HIF-1)-target genes that form the core response to hypoxia. Nucleic Acids Res 37(14):4587–4602

Carmeliet P, Dor Y, Herbert JM, Fukumura D, Brusselmans K, Dewerchin M, Neeman M, Bono F, Abramovitch R, Maxwell P, Koch CJ, Ratcliffe P, Moons L, Jain RK, Collen D, Keshert E (1998) Role of HIF-1alpha in hypoxia-mediated apoptosis, cell proliferation and tumour angiogenesis. Nature 394(6692):485–490

Davuluri RV, Suzuki Y, Sugano S, Plass C, Huang TH (2008) The functional consequences of alternative promoter use in mammalian genomes. Trends Genet 24(4):167–177

Forsythe JA, Jiang BH, Iyer NV, Agani F, Leung SW, Koos RD, Semenza GL (1996) Activation of vascular endothelial growth factor gene transcription by hypoxia-inducible factor 1. Mol Cell Biol 16(9):4604–4613

Fraisl P, Aragones J, Carmeliet P (2009) Inhibition of oxygen sensors as a therapeutic strategy for ischaemic and inflammatory disease. Nat Rev Drug Discov 8(2):139–152

Fyles AW, Milosevic M, Wong R, Kavanagh MC, Pintilie M, Sun A, Chapman W, Levin W, Manchul L, Keane TJ, Hill RP (1998) Oxygenation predicts radiation response and survival in patients with cervix cancer. Radiother Oncol 48(2):149–156

Gatenby RA, Gillies RJ (2004) Why do cancers have high aerobic glycolysis? Nat Rev Cancer 4(11):891–899

Gerhard DS, Wagner L, Feingold EA, Shenmen CM, Grouse LH, Schuler G, Klein SL, Old S, Rasooly R, Good P, Guyer M, Peck

AM, Derge JG, Lipman D, Collins FS, Jang W, Sherry S, Feolo M, Misquitta L, Lee E, Rotmistrovsky K, Greenhut SF, Schaefer CF, Buetow K, Bonner TI, Haussler D, Kent J, Kiekhaus M, Furey T, Brent M, Prange C, Schreiber K, Shapiro N, Bhat NK, Hopkins RF, Hsie F, Driscoll T, Soares MB, Casavant TL, Scheetz TE, Brown-stein MJ, Usdin TB, Toshiyuki S, Carninci P, Piao Y, Dudekula DB, Ko MS, Kawakami K, Suzuki Y, Sugano S, Gruber CE, Smith MR, Simmons B, Moore T, Waterman R, Johnson SL, Ruan Y, Wei CL, Mathavan S, Gunaratne PH, Wu J, Garcia AM, Hulyk SW, Fuh E, Yuan Y, Sneed A, Kowis C, Hodgson A, Muzny DM, McPherson J, Gibbs RA, Fahey J, Helton E, Ketteman M, Madan A, Rodrigues S, Sanchez A, Whiting M, Madari A, Young AC, Wetherby KD, Granite SJ, Kwong PN, Brinkley CP, Pearson RL, Bouffard GG, Blakesly RW, Green ED, Dickson MC, Rodriguez AC, Grimwood J, Schmutz J, Myers RM, Butterfield YS, Griffith M, Griffith OL, Krzywinski MI, Liao N, Morin R, Palmquist D, Petrescu AS, Skalska U, Smailus DE, Stott JM, Schnerch A, Schein JE, Jones SJ, Holt RA, Baross A, Marra MA, Clifton S, Makowski KA, Bosak S, Malek J (2004) The status, quality, and expansion of the NIH full-length cDNA project: the Mammalian Gene Collection (MGC). Genome Res 14(10B):2121–2127

Griffiths-Jones S, Grocock RJ, van Dongen S, Bateman A, Enright AJ (2006) miRBase: microRNA sequences, targets and gene nomenclature. Nucleic Acids Res 34(Database issue):D140–D144

Guttman M, Amit I, Garber M, French C, Lin MF, Feldser D, Huarte M, Zuk O, Carey BW, Cassady JP, Cabili MN, Jaenisch R, Mikkelsen TS, Jacks T, Hacohen N, Bernstein BE, Kellis M, Regev A, Rinn JL, Lander ES (2009) Chromatin signature reveals over a thousand highly conserved large non-coding RNAs in mammals. Nature 458(7235):223–227

Harris AL (2002) Hypoxia—a key regulatory factor in tumour growth. Nat Rev Cancer 2(1):38–47

He L, Hannon GJ (2004) MicroRNAs: small RNAs with a big role in gene regulation. Nat Rev Genet 5(7):522–531

Heintzman ND, Stuart RK, Hon G, Fu Y, Ching CW, Hawkins RD, Barrera LO, Van Calcar S, Qu C, Ching KA, Wang W, Weng Z, Green RD, Crawford GE, Ren B (2007) Distinct and predictive chromatin signatures of transcriptional promoters and enhancers in the human genome. Nat Genet 39(3):311–318

Hirota K, Semenza GL (2006) Regulation of angiogenesis by hypoxia-inducible factor 1. Crit Rev Oncol Hematol 59(1):15–26

Jiang C, Pugh BF (2009) Nucleosome positioning and gene regulation: advances through genomics. Nat Rev Genet 10(3):161–172

Keith B, Simon MC (2007) Hypoxia-inducible factors, stem cells, and cancer. Cell 129(3):465–472

Kim J, Chu J, Shen X, Wang J, Orkin SH (2008) An extended transcriptional network for pluripotency of embryonic stem cells. Cell 132(6):1049–1061

Koritzinsky M, Wouters BG (2007) Hypoxia and regulation of messenger RNA translation. Methods Enzymol 435:247–273

Kwon H, Thierry-Mieg D, Thierry-Mieg J, Kim HP, Oh J, Tunyaplin C, Carotta S, Donovan CE, Goldman ML, Tailor P, Ozato K, Levy DE, Nutt SL, Calame K, Leonard WJ (2009) Analysis of interleukin-21-induced Prdm1 gene regulation reveals functional cooperation of STAT3 and IRF4 transcription factors. Immunity 31(6):941–952

Landry JR, Mager DL, Wilhelm BT (2003) Complex controls: the role of alternative promoters in mammalian genomes. Trends Genet 19(11):640–648

Lin B, Wang J, Hong X, Yan X, Hwang D, Cho JH, Yi D, Utleg AG, Fang X, Schones DE, Zhao K, Omenn GS, Hood L (2009) Integrated expression profiling and ChIP-seq analyses of the growth inhibition response program of the androgen receptor. PLoS One 4(8):e6589

Maxwell PH (2005) The HIF pathway in cancer. Semin Cell Dev Biol 16(4–5):523–530

Mole DR, Blancher C, Copley RR, Pollard PJ, Gleadle JM, Ragoussis J, Ratcliffe PJ (2009) Genome-wide association of hypoxia-inducible factor (HIF)-1alpha and HIF-2alpha DNA binding with expression profiling of hypoxia-inducible transcripts. J Biol Chem 284(25):16767–16775

Nishi H, Nakada T, Kyo S, Inoue M, Shay JW, Isaka K (2004) Hypoxia-inducible factor 1 mediates upregulation of telomerase (hTERT). Mol Cell Biol 24(13):6076–6083

Nordsmark M, Overgaard M, Overgaard J (1996) Pretreatment oxygenation predicts radiation response in advanced squamous cell carcinoma of the head and neck. Radiother Oncol 41(1):31–39

Ortiz-Barahona A, Villar D, Pescador N, Amigo J, del Peso L (2010) Genome-wide identification of hypoxia-inducible factor binding sites and target genes by a probabilistic model integrating transcription-profiling data and in silico binding site prediction. Nucleic Acids Res 38(7):2332–2345

Ota T, Suzuki Y, Nishikawa T, Otsuki T, Sugiyama T, Irie R, Wakamatsu A, Hayashi K, Sato H, Nagai K, Kimura K, Makita H, Sekine M, Obayashi M, Nishi T, Shibahara T, Tanaka T, Ishii S, Yamamoto J, Saito K, Kawai Y, Isono Y, Nakamura Y, Nagahari K, Murakami K, Yasuda T, Iwayanagi T, Wagatsuma M, Shiratori A, Sudo H, Hosoiri T, Kaku Y, Kodaira H, Kondo H, Sugawara M, Takahashi M, Kanda K, Yokoi T, Furuya T, Kikkawa E, Omura Y, Abe K, Kamihara K, Katsuta N, Sato K, Tanikawa M, Yamazaki M, Ninomiya K, Ishibashi T, Yamashita H, Murakawa K, Fujimori K, Tanai H, Kimata M, Watanabe M, Hiraoka S, Chiba Y, Ishida S, Ono Y, Takiguchi S, Watanabe S, Yosida M, Hotuta T, Kusano J, Kanehori K, Takahashi-Fujii A, Hara H, Tanase TO, Nomura Y, Togiya S, Komai F, Hara R, Takeuchi K, Arita M, Imose N, Musashino K, Yuuki H, Oshima A, Sasaki N, Aotsuka S, Yoshikawa Y, Matsunawa H, Ichihara T, Shiohata N, Sano S, Moriya S, Momiyama H, Satoh N, Takami S, Terashima Y, Suzuki O, Nakagawa S, Senoh A, Mizoguchi H, Goto Y, Shimizu F, Wakebe H, Hishigaki H, Watanabe T, Sugiyama A, Takemoto M, Kawakami B, Yamazaki M, Watanabe K, Kumagai A, Itakura S, Fukuzumi Y, Fujimori Y, Komiyama M, Tashiro H, Tanigami A, Fujiwara T, Ono T, Yamada K, Fujii Y, Ozaki K, Hirao M, Ohmori Y, Kawabata A, Hikiji T, Kobatake N, Inagaki H, Ikema Y, Okamoto S, Okitani R, Kawakami T, Noguchi S, Itoh T, Shigeta K, Senba T, Matsumura K, Nakajima Y, Mizuno T, Morinaga M, Sasaki M, Togashi T, Oyama M, Hata H, Watanabe M, Komatsu T, Mizushima-Sugano J, Satoh T, Shirai Y, Takahashi Y, Nakagawa K, Okumura K, Nagase T, Nomura N, Kikuchi H, Masuho Y, Yamashita R, Nakai K, Yada T, Nakamura Y, Ohara O, Isogai T, Sugano S (2004) Complete sequencing and characterization of 21,243 full-length human cDNAs. Nat Genet 36(1):40–45

Park PJ (2009) ChIP-seq: advantages and challenges of a maturing technology. Nat Rev Genet 10(10):669–680

Polak P, Domany E (2006) Alu elements contain many binding sites for transcription factors and may play a role in regulation of developmental processes. BMC Genomics 7:133

Poon E, Harris AL, Ashcroft M (2009) Targeting the hypoxia-inducible factor (HIF) pathway in cancer. Expert Rev Mol Med 11:e26

Pouyssegur J, Dayan F, Mazure NM (2006) Hypoxia signalling in cancer and approaches to enforce tumour regression. Nature 441(7092):437–443

Rajaganeshan R, Prasad R, Guillou PJ, Scott N, Poston G, Jayne DG (2009) Expression patterns of hypoxic markers at the invasive margin of colorectal cancers and liver metastases. Eur J Surg Oncol 35(12):1286–1294

Raval RR, Lau KW, Tran MG, Sowter HM, Mandriota SJ, Li JL, Pugh CW, Maxwell PH, Harris AL, Ratcliffe PJ (2005) Contrasting properties of hypoxia-inducible factor 1 (HIF-1) and HIF-2 in von Hippel-Lindau-associated renal cell carcinoma. Mol Cell Biol 25(13):5675–5686

Robertson G, Hirst M, Bainbridge M, Bilenky M, Zhao Y, Zeng T, Euskirchen G, Bernier B, Varhol R, Delaney A, Thiessen N, Griffith OL, He A, Marra M, Snyder M, Jones S (2007) Genome-wide profiles of STAT1 DNA association using chromatin immunoprecipitation and massively parallel sequencing. Nat Methods 4(8):651–657

Schmitz KJ, Muller CI, Reis H, Alakus H, Winde G, Baba HA, Wohlschlaeger J, Jasani B, Fandrey J, Schmid KW (2009) Combined analysis of hypoxia-inducible factor 1 alpha and metallothionein indicates an aggressive subtype of colorectal carcinoma. Int J Colorectal Dis 24(11):1287–1296

Schones DE, Cui K, Cuddapah S, Roh TY, Barski A, Wang Z, Wei G, Zhao K (2008) Dynamic regulation of nucleosome positioning in the human genome. Cell 132(5):887–898

Semenza GL (2000) HIF-1 and human disease: one highly involved factor. Genes Dev 14(16):1983–1991

Semenza GL (2003) Targeting HIF-1 for cancer therapy. Nat Rev Cancer 3(10):721–732

Semenza GL (2010) Defining the role of hypoxia-inducible factor 1 in cancer biology and therapeutics. Oncogene 29(5):625–634

Semenza GL, Wang GL (1992) A nuclear factor induced by hypoxia via de novo protein synthesis binds to the human erythropoietin gene enhancer at a site required for transcriptional activation. Mol Cell Biol 12(12):5447–5454

Thomas JD, Johannes GJ (2007) Identification of mRNAs that continue to associate with polysomes during hypoxia. Rna 13(7): 1116–1131

Tian H, McKnight SL, Russell DW (1997) Endothelial PAS domain protein 1 (EPAS1), a transcription factor selectively expressed in endothelial cells. Genes Dev 11(1):72–82

Tomilin NV (2008) Regulation of mammalian gene expression by retroelements and non-coding tandem repeats. Bioessays 30(4): 338–348

Tsuchihara K, Suzuki Y, Wakaguri H, Irie T, Tanimoto K, Hashimoto S, Matsushima K, Mizushima-Sugano J, Yamashita R, Nakai K, Bentley D, Esumi H, Sugano S (2009) Massive transcriptional start site analysis of human genes in hypoxia cells. Nucleic Acids Res 37(7):2249–2263

Valouev A, Johnson DS, Sundquist A, Medina C, Anton E, Batzoglou S, Myers RM, Sidow A (2008) Genome-wide analysis of transcription factor binding sites based on ChIP-Seq data. Nat Methods 5(9):829–834

Wang GL, Semenza GL (1995) Purification and characterization of hypoxia-inducible factor 1. J Biol Chem 270(3):1230–1237

Welboren WJ, van Driel MA, Janssen-Megens EM, van Heeringen SJ, Sweep FC, Span PN, Stunnenberg HG (2009) ChIP-Seq of ERalpha and RNA polymerase II defines genes differentially responding to ligands. EMBO J 28(10):1418–1428

Wenger RH, Kvietikova I, Rolfs A, Camenisch G, Gassmann M (1998) Oxygen-regulated erythropoietin gene expression is dependent on a CpG methylation-free hypoxia-inducible factor-1 DNA-binding site. Eur J Biochem 253(3):771–777

Wenger RH, Stiehl DP, Camenisch G (2005) Integration of oxygen signaling at the consensus HRE. Sci STKE (306):re12

Wiesener MS, Jurgensen JS, Rosenberger C, Scholze CK, Horstrup JH, Warnecke C, Mandriota S, Bechmann I, Frei UA, Pugh CW, Ratcliffe PJ, Bachmann S, Maxwell PH, Eckardt KU (2003) Widespread hypoxia-inducible expression of HIF-2alpha in distinct cell populations of different organs. Faseb J 17(2):271–273

Wilusz JE, Sunwoo H, Spector DL (2009) Long noncoding RNAs: functional surprises from the RNA world. Genes Dev 23(13): 1494–1504

Xia X, Kung AL (2009) Preferential binding of HIF-1 to transcriptionally active loci determines cell-type specific response to hypoxia. Genome Biol 10(10):R113

Xia X, Lemieux ME, Li W, Carroll JS, Brown M, Liu XS, Kung AL (2009) Integrative analysis of HIF binding and transactivation reveals its role in maintaining histone methylation homeostasis. Proc Natl Acad Sci U S A 106(11):4260–4265

Zhang Y, Moqtaderi Z, Rattner BP, Euskirchen G, Snyder M, Kadonaga JT, Liu XS, Struhl K (2009) Intrinsic histone-DNA interactions are not the major determinant of nucleosome positions in vivo. Nat Struct Mol Biol 16(8):847–852

British Journal of Cancer (2011) 105, 403–406

www.bjcancer.com

KRAS mutations detected by the amplification refractory mutation system–Scorpion assays strongly correlate with therapeutic effect of cetuximab

H Bando[1,2], T Yoshino*[,1], K Tsuchihara[2], N Ogasawara[2], N Fuse[1], T Kojima[1], M Tahara[1], M Kojima[3], K Kaneko[1], T Doi[1], A Ochiai[3], H Esumi[2] and A Ohtsu[1]

[1]Department of Gastroenterology and Gastrointestinal Oncology, National Cancer Center Hospital East, 6-5-1 Kashiwanoha, Kashiwa, Chiba 277-8577, Japan; [2]Cancer Physiology Project, Research Center for Innovative Oncology, National Cancer Center Hospital East, 6-5-1 Kashiwanoha, Kashiwa, Chiba 277-8577, Japan; [3]Pathology Division, Research Center for Innovative Oncology, National Cancer Center Hospital East, 6-5-1 Kashiwanoha, Kashiwa, Chiba 277-8577, Japan

BACKGROUND: We aimed to compare the sensitive and quality-controlled *KRAS* testing with direct sequencing and to assess the impact on decision making of treatment.

PATIENTS AND METHODS: We analysed genomic DNA isolated from macrodissected formalin-fixed paraffin-embedded specimens by direct sequencing and an amplification refractory mutation system–Scorpion assay (ARMS/S) method. Cetuximab was administered to patients identified as having wild-type (WT) *KRAS* using direct sequencing. Therapeutic effects were evaluated according to their *KRAS* status as determined by ARMS/S.

RESULTS: Among the 159 patients, the overall mutation rate was determined to be 37.0% by direct sequencing and 44.0% by ARMS/S. For the patients diagnosed as WT by direct sequencing and treated with cetuximab ($n=47$), a response rate of 16.0% was observed for 38 ARMS/S WT patients, whereas 9 ARMS/S mutant (MUT) patients failed to respond. The ARMS/S WT patients showed significant improvement in progression-free survival (PFS) and overall survival (OS) compared with ARMS/S MUT patients (PFS median 5.0 *vs* 1.7 months, hazards ratio (HR) = 0.29, $P=0.001$; OS median 12.1 *vs* 3.8 months, HR = 0.26, $P=0.001$).

CONCLUSION: Sensitive and quality-controlled *KRAS* testing may provide improved predictive power to determine the efficacy of anti-epidermal growth factor antibodies.

British Journal of Cancer (2011) **105,** 403–406. doi:10.1038/bjc.2011.247 www.bjcancer.com
Published online 5 July 2011

Keywords: ARMS/S; colorectal cancer; direct sequencing; formalin-fixed paraffin-embedded specimen; *KRAS*

Retrospective subset analyses and prospective randomised phase III clinical trials have suggested that anti-epidermal growth factor antibodies do not benefit patients with metastatic colorectal cancer harbouring *KRAS* mutations (Amado *et al*, 2008; Karapetis *et al*, 2008; Tol *et al*, 2009; Van Cutsem *et al*, 2009). On the basis of these findings, regulatory authorities in Europe, the United States and Japan require pretreatment *KRAS* mutation testing. In Europe, the KRAS European Quality Assurance Program (http://kras.eqascheme.org/) has been launched and several Communauté Européene-labelled *KRAS* mutation test kits such as the TheraScreen K-RAS Mutation Kit (DxS-QIAGEN, Manchester, UK), KRAS LightMix (TIB MolBiol, Berlin, Germany) and PyroMark Q24 KRAS Kit (QIAGEN, Duesseldorf, Germany) have been approved for diagnostic use. The TheraScreen Kit combines the amplification refractory mutation system (ARMS) with a unique bifunctional fluorescent primer/probe molecule (Scorpion) and is recommended for clinical use because of its high sensitivity, robustness and convenience (Franklin *et al*, 2009; Jimeno *et al*, 2009; Kotoula *et al*, 2009; Whitehall *et al*, 2009; Angulo *et al*, 2010; Ogasawara *et al*, 2011).

Together with these standardised methods, direct sequencing is still one of the most accessible methods. However, several critical disadvantages of direct sequencing for diagnostic use have been indicated. These include its low sensitivity and lack of strict criteria for distinguishing mutant signals from contaminated noises. Furthermore, we have recently reported that insufficient PCR amplification further limits the sensitivity and specificity of direct sequencing. This is particularly important when DNA isolated from formalin-fixed paraffin-embedded (FFPE) specimens, which contain low levels of amplifiable DNA, is used (Bando *et al*, 2011). To increase the sensitivity of direct sequencing, macroscopic isolation of tissues in which cancer cells occupy >70% of the area (macrodissection) is recommended for preparation of genomic DNA (Kotoula *et al*, 2009).

Although discrepancies in interpretation between the ARMS–Scorpion assay (ARMS/S) and direct sequencing have been noted, the impact of these discrepancies on treatment has not been adequately evaluated (Franklin *et al*, 2009; Kotoula *et al*, 2009). In this study, we evaluated the validity of ARMS/S and direct

*Correspondence: Dr T Yoshino; E-mail: tyoshino@east.ncc.go.jp
Received 1 March 2011; revised 6 June 2011; accepted 7 June 2011; published online 5 July 2011

sequencing by comparing the therapeutic effects of cetuximab in patients in whom *KRAS* mutations were analysed by these two methods.

PATIENTS AND METHODS

DNA samples and *KRAS* mutation testing

Genomic DNA was extracted from primary and metastatic colorectal cancer tissues of patients scheduled to receive cetuximab. DNA extraction from FFPE tissue blocks has been previously described. The *KRAS* exon-2 fragment was amplified and sequenced according to previously described methods (Bando *et al*, 2011). The *KRAS* PCR Kit (DxS-QIAGEN) was used for detection of seven major mutations in *KRAS* codons 12 and 13. Reactions were performed using the LightCycler 480 Real-Time PCR System (Roche Diagnostics, Mannheim, Germany) and analysed with LightCycler Adapt software v1.1 (Roche Diagnostics) as previously described (Bando *et al*, 2011).

Patients

Cetuximab was administered at the National Cancer Center Hospital East (NCCHE) in patients diagnosed with wild-type (WT) *KRAS* by direct sequencing. Furthermore, *KRAS* mutation status was evaluated using ARMS/S.

Patients who met all inclusion criteria were retrospectively included in analyses. Inclusion criteria were as follows: (1) age $\geqslant$20 years; (2) histologically confirmed adenocarcinoma of the colon or rectum; (3) presence of unresectable metastatic disease; (4) baseline computed tomography (CT) scan performed within the previous 28 days; (5) initial evaluation by CT scan within 3 months; (6) documentation of refractory to previous fluoropyrimidine, oxaliplatin and irinotecan administration; (7) *KRAS* mutational status determined by direct sequencing and ARMS/S; (8) Eastern Cooperative Oncology Group performance status score $\leqslant$2; (9) adequate haematological, hepatic, renal and bone marrow function; and (10) undergone treatment with cetuximab monotherapy regimen or combination regimen with cetuximab plus irinotecan. In the monotherapy regimen, cetuximab was administered at an initial dose of 400 mg m^{-2}, followed by weekly infusions of 250 mg m^{-2}. In the combination regimen, cetuximab was administered at the same dose as for monotherapy, followed by biweekly infusions of 150 mg m^{-2} irinotecan.

The study was conducted with the approval of the institutional review board.

Measured outcomes

The therapeutic response rate was evaluated according to the Response Evaluation Criteria in Solid Tumours (version 1.0). Progression-free survival (PFS) was defined as the time from the first cetuximab administration to either first objective evidence of disease progression or death from any cause. Overall survival (OS) was defined as the time from the first administration of cetuximab to death from any cause.

Statistical analysis

The response rate, PFS and OS of all patients were revalued for this study. Fisher's exact test and the Mann–Whitney test were used to compare the patient characteristics and response rates. The PFS and OS data were plotted as Kaplan–Meier curves and the differences between the groups categorised by ARMS/S-identified *KRAS* status were compared by the log-rank test. The hazard ratio (HR) was calculated from the Cox regression model with a single covariate. All analyses were performed using IBM SPSS Statistics 18 package software (SPSS Inc., Tokyo, Japan).

RESULTS

Mutation rates determined by direct sequencing and ARMS/S

From April 2009 to March 2010, 159 specimens were tested using both ARMS/S and direct sequencing (98 specimens were collected from NCCHE and 61 from other hospitals). Both methods had a success rate of 100%. In all, 59 (37.0%) *KRAS* mutations were detected by direct sequencing and 70 (44.0%) by ARMS/S (Table 1a). All mutations identified by direct sequencing were also identified by ARMS/S. However, 11 (7.0%) of the 70 *KRAS* mutations identified by ARMS/S were not detected by direct sequencing. The overall concordance rate of the two methods was 93.0% (Table 1b).

Patient characteristics

From April 2009 to March 2010, 47 patients met with all of the inclusion criteria (11 patients were treated with cetuximab monotherapy and 36 patients were treated with cetuximab plus irinotecan). Of the 47 patients, 38 and 9 patients were identified by ARMS/S as WT (ARMS/S WT) and mutant (ARMS/S MUT), respectively (Table 2). Patient characteristics of the two groups (ARMS/S WT *vs* ARMS/S MUT) were not significantly different except for the incidence of lung metastases (Table 2).

Response to treatment

The response rate of ARMS/S WT patients was 16.0%. In contrast, no objective tumour response was observed in ARMS/S MUT patients. In addition, the disease control rates (including partial response and stable disease) of ARMS/S WT and ARMS/S MUT patients were 66.0% and 56.0%, respectively (Table 3).

Survival

The median PFS of the 38 ARMS/S WT and 9 ARMS/S MUT patients was 5.0 and 1.7 months, respectively (HR = 0.29, P = 0.001; Table 3 and Figure 1A). The relative dose intensity of cetuximab therapy was not significantly different between ARMS/S WT and ARMS/S MUT patients (Table 3). The median OS of the 38 ARMS/S WT and 9 ARMS/S MUT patients was 12.1 and 3.8 months, respectively (HR = 0.26, P = 0.001; Table 3 and Figure 1B).

When the patients were divided as per treatment regimen, the median PFS and OS of the patients treated with cetuximab plus

Table 1a Comparison of mutation detection techniques

Method	Direct sequencing	ARMS/S
Success rate	100% (159 out of 159)	100% (159 out of 159)
Mutation rate	37.0% (59 out of 159)	44.0% (70 out of 159)

Abbreviation: ARMS/S = amplification refractory mutation system–Scorpion assay.

Table 1b Pairwise comparisons of mutation detection frequency

	Direct sequencing		
ARMS/S	WT	MUT	Total
WT	89 (56.0%)	0 (0%)	89 (56.0%)
MUT	11 (7.0%)	59 (37.0%)	70 (44.0%)
Total	100 (63.0%)	59 (37.0%)	159 (100%)

Abbreviations: ARMS/S = amplification refractory mutation system-Scorpion assay; MUT = mutant; WT = wild type.

Table 2 Patient characteristics

Characteristic	DS WT ARMS/S WT ($n=38$)	DS WT ARMS/S MUT ($n=9$)	*P*-value
Treatment (cetuximab monotherapy/ cetuximab+irinotecan)	8/30	3/6	0.350[a]
Age (median)	65	66	0.234[b]
Sex (M/F)	26/12	6/3	0.604[a]
ECOG PS (0/1or 2)	29/9	4/5	0.740[a]
Site of primary cancer (right/left/rectum)	17/10/11	1/3/4	0.401[a]
Histologic appearance (well diff./poorly diff.)	34/4	9/0	0.414[a]
Metastatic site			
Liver (%)	47.0	44.0	0.586[a]
Lung (%)	47.0	89.0	0.026[a]
Nodes (%)	47.0	78.0	0.100[a]
Ascites (%)	21.0	11.0	0.433[a]
No. of metastatic sites (1/>2)	19/19	2/7	0.128[a]

Abbreviations: ARMS/S = amplification refractory mutation system–Scorpion assay; DS = direct sequencing; ECOG PS = Eastern Cooperative Oncology Group Performance Status Scale; F = female; M = male; MUT = mutant; WT = wild type. [a]One-tailed Fisher's exact test. [b]Mann-Whitney test.

Table 3 Efficacy and relative dose intensity in the test population according to *KRAS* status determined by ARMS/S

Characteristic	DS WT ARMS/S WT ($n=38$)	DS WT ARMS/S MUT ($n=9$)
Partial response	6	0
Stable disease	19	5
Progressive disease	13	4
Response rate	16.0%[a]	0%[a]
Disease control rate	66.0%	56.0%
Progression-free survival, median (months)	5.0	1.7
Overall survival, median (months)	12.1	3.8
Relative dose intensity		
Cetuximab, median (range)	0.94 (0.57–1.00)	0.93 (0.57–1.00)

Abbreviations: ARMS/S = amplification refractory mutation system–Scorpion assay; DS = direct sequencing; MUT = mutant; WT = wild type. [a]$P=0.257$ (one-tailed Fisher's exact test).

irinotecan were significantly different from ARMS/S WT and ARMS/S MUT patients (PFS; HR = 0.23, $P=0.002$, OS; HR = 0.187, $P=0.001$). Similar trends were also observed for the patients treated with cetuximab monotherapy (PFS; HR = 0.497, $P=0.332$, OS; HR = 0.674, $P=0.586$).

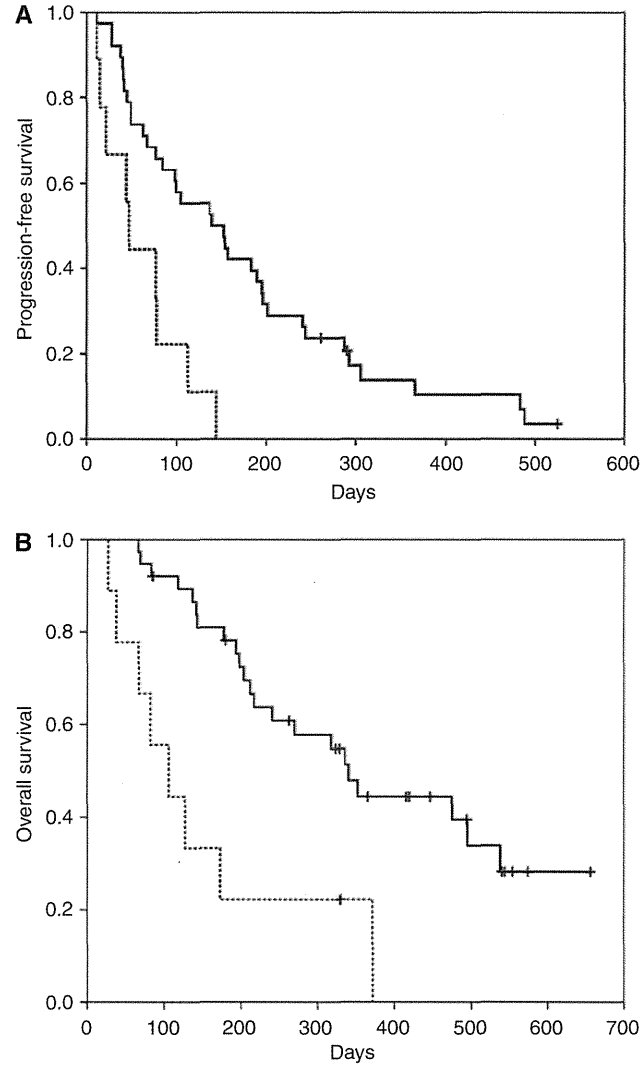

Figure 1 (**A**) Kaplan–Meier plots of progression-free survival (PFS) according to *KRAS* status determined by the amplification refractory mutation system–Scorpion assay (ARMS/S). For the patients treated with cetuximab-containing regimens, the median PFS values were 5.0 and 1.7 months for ARMS/S wild-type (solid line) and ARMS/S mutant (dashed line) patients, respectively. The difference was statistically significant (HR = 0.29, $P=0.001$). (**B**) Kaplan–Meier plots of overall survival (OS) according to *KRAS* status determined by ARMS/S. For the patients treated with cetuximab-containing regimens, the median OS values for ARMS/S wild-type (solid line) and ARMS/S mutant (dashed line) patients were 12.1 and 3.8 months, respectively. The difference was statistically significant (HR = 0.26, $P=0.001$).

DISCUSSION

The present guidelines for *KRAS* testing allow direct sequencing for MUT detection (Allegra *et al*, 2009). To overcome the low sensitivity of direct sequencing, we performed macrodissection of the tissues in order to enrich the tumour cell-derived DNA. We also improved the PCR conditions based on our previous study (Bando *et al*, 2011). The mutation rates determined by direct sequencing in the present study were comparable with those reported in previous studies (36.0–43.0%) as per various mutation detection methods, including ARMS/S, and thus support the validity of our direct sequencing procedure (Amado *et al*, 2008; Karapetis *et al*, 2008; Tol *et al*, 2009; Van Cutsem *et al*, 2009). In contrast, the mutation rate determined using simultaneous ARMS/S appeared to be higher than that found in previous clinical trials (Amado *et al*, 2008; Karapetis *et al*, 2008; Tol *et al*, 2009; Van Cutsem *et al*, 2009). Therefore, we surmise that enrichment of tumour cell-derived DNA may further enhance the sensitivity of ARMS/S.

Next, we examined whether this higher sensitivity could result in improved clinical relevance. The median PFS, OS and response rates of *KRAS* WT patients determined by ARMS/S were

comparable with those previously reported (median PFS, 3.8 months; median OS, 9.5 months; response rate, 13.0%) (Karapetis *et al*, 2008). In contrast, the median PFS, OS and response rates of the *KRAS* MUT patients, although determined as WT by direct sequencing, were comparable with those of MUT *KRAS* patients reported in previous clinical trials (median PFS, 1.8 months; median OS, 4.5 months; response rate, 1.0%) (Karapetis *et al*, 2008).

Two factors may be responsible for the significant advantage of ARMS/S. First, the higher sensitivity of the ARM/S assay can detect the presence of a lesser number of *KRAS* mutations than direct sequencing. Second, strictly controlled criteria for MUT identification provided robust detection and eliminated the 'grey zone' cases that we often encountered using direct sequencing.

On the other hand, the intratumoral heterogeneity of tumour tissues for *KRAS* gene status suggested that residual *KRAS* WT tumour cells may respond to cetuximab, but this idea is still under debate (Baldus *et al*, 2010). In the present study, although ARMS/S MUT patients showed poorer PFS and OS than the WT patients, 5 of the 9 patients achieved disease stability in the first CT evaluation. Although this study had limitations such as small sample size and retrospective design that could have caused substantial biases, it appears that tumour heterogeneity allowed a reasonable level of disease control. Thus, further evaluation with an adequate sample size, in a prospective manner, would be required to determine which of the testing methods (direct sequencing or ARMS/S) would be a better predictive marker for clinical benefits.

In conclusion, our study suggested that *KRAS* mutation status determined by ARMS/S appeared to be more closely related to clinical effects than that determined by direct sequencing, although there were limitations of sample size and retrospective design. Whether *KRAS* mutation status determined by ARMS/S can be used as a predictive biomarker is not yet known. However, the study results warrant further investigation of this method, which should evaluate the correlations between *KRAS* mutation status and clinical outcomes in comparison with those achieved by direct sequencing.

ACKNOWLEDGEMENTS

This work was partly supported by 'Grants for the Third-Term Comprehensive 10-Year Strategy for Cancer Control' and 'Grant-in-Aid for Cancer Research from the Ministry of Health, Labor and Welfare, Japan'.

Conflict of interest

The authors declare no conflict interest.

REFERENCES

Allegra CJ, Jessup JM, Somerfield MR, Hamilton SR, Hammond EH, Hayes DF, McAllister PK, Morton RF, Schilsky RL (2009) American Society of Clinical Oncology provisional clinical opinion: testing for KRAS gene mutations in patients with metastatic colorectal carcinoma to predict response to anti-epidermal growth factor receptor monoclonal antibody therapy. *J Clin Oncol* **27:** 2091–2096

Amado RG, Wolf M, Peeters M, Van Cutsem E, Siena S, Freeman DJ, Juan T, Sikorski R, Suggs S, Radinsky R, Patterson SD, Chang DD (2008) Wild-type KRAS is required for panitumumab efficacy in patients with metastatic colorectal cancer. *J Clin Oncol* **26:** 1626–1634

Angulo B, Garcia-Garcia E, Martinez R, Suarez-Gauthier A, Conde E, Hidalgo M, Lopez-Rios F (2010) A commercial real-time PCR kit provides greater sensitivity than direct sequencing to detect KRAS mutations: a morphology-based approach in colorectal carcinoma. *J Mol Diagn* **12:** 292–299

Baldus SE, Schaefer KL, Engers R, Hartleb D, Stoecklein NH, Gabbert HE (2010) Prevalence and heterogeneity of KRAS, BRAF and PIK3CA mutations in primary colorectal adenocarcinomas and their corresponding metastases. *Clin Cancer Res* **16:** 790–799

Bando H, Tsuchihara K, Yoshino T, Kojima M, Ogasawara N, Fukushima H, Ochiai A, Ohtsu A, Esumi H (2011) Biased discordance of KRAS mutation detection in archived colorectal cancer specimens between the ARMS-Scorpion method and direct sequencing. *Jpn J Clin Oncol* **41:** 239–244

Franklin WA, Haney J, Sugita M, Bemis L, Jimeno A, Messersmith WA (2009) KRAS mutation: comparison of testing methods and tissue sampling techniques in colon cancer. *J Mol Diagn* **12:** 43–50

Jimeno A, Messersmith WA, Hirsch FR, Franklin WA, Eckhardt SG (2009) KRAS mutations and sensitivity to epidermal growth factor receptor inhibitors in colorectal cancer: practical application of patient selection. *J Clin Oncol* **27:** 1130–1136

Karapetis CS, Khambata-Ford S, Jonker DJ, O'Callaghan CJ, Tu D, Tebbutt NC, Simes RJ, Chalchal H, Shapiro JD, Robitaille S, Price TJ, Shepherd L, Au HJ, Langer C, Moore MJ, Zalcberg JR (2008) K-ras mutations and benefit from cetuximab in advanced colorectal cancer. *N Engl J Med* **359:** 1757–1765

Kotoula V, Charalambous E, Biesmans B, Malousi A, Vrettou E, Fountzilas G, Karkavelas G (2009) Targeted KRAS mutation assessment on patient tumour histologic material in real time diagnostics. *PLoS ONE* **4:** e7746

Ogasawara N, Bando H, Kawamoto Y, Yoshino T, Tsuchihara K, Ohtsu A, Esumi H (2011) Feasibility and robustness of amplification refractory mutation system (ARMS)-based KRAS testing using clinically available formalin-fixed, paraffin-embedded samples of colorectal cancers. *Jpn J Clin Oncol* **41:** 52–56

Tol J, Koopman M, Cats A, Rodenburg CJ, Creemers GJ, Schrama JG, Erdkamp FL, Vos AH, van Groeningen CJ, Sinnige HA, Richel DJ, Voest EE, Dijkstra JR, Vink-Borger ME, Antonini NF, Mol L, van Krieken JH, Dalesio O, Punt CJ (2009) Chemotherapy, bevacizumab and cetuximab in metastatic colorectal cancer. *N Engl J Med* **360:** 563–572

Van Cutsem E, Kohne CH, Hitre E, Zaluski J, Chang Chien CR, Makhson A, D'Haens G, Pinter T, Lim R, Bodoky G, Roh JK, Folprecht G, Ruff P, Stroh C, Tejpar S, Schlichting M, Nippgen J, Rougier P (2009) Cetuximab and chemotherapy as initial treatment for metastatic colorectal cancer. *N Engl J Med* **360:** 1408–1417

Whitehall V, Tran K, Umapathy A, Grieu F, Hewitt C, Evans TJ, Ismail T, Li WQ, Collins P, Ravetto P, Leggett B, Salto-Tellez M, Soong R, Fox S, Scott RJ, Dobrovic A, Iacopetta B (2009) A multicenter blinded study to evaluate KRAS mutation testing methodologies in the clinical setting. *J Mol Diagn* **11:** 543–552

PHYTOTHERAPY RESEARCH
Phytother. Res. **25**: 1770–1775 (2011)
Published online 6 April 2011 in Wiley Online Library
(wileyonlinelibrary.com) **DOI**: 10.1002/ptr.3441

Identification of Chrysoplenetin from *Vitex negundo* as a Potential Cytotoxic Agent against PANC-1 and a Panel of 39 Human Cancer Cell Lines (JFCR-39)

Suresh Awale,[1]* Thein Zaw Linn,[1,2] Feng Li,[1] Yasuhiro Tezuka,[1] Aung Myint,[2] Akihiro Tomida,[3] Takao Yamori,[4] Hiroyasu Esumi[5] and Shigetoshi Kadota[1]*

[1]Institute of Natural Medicine, University of Toyama, 2630-Sugitani, Toyama 930-0194, Japan
[2]University of Traditional Medicine, Aung Myay ThaSan tsp, Mandalay, Union of Myanmar
[3]Division of Genome Research, Cancer Chemotherapy Center, Japanese Foundation for Cancer Research, 3-8-31 Ariake, Koto-ku, 135-8550 Tokyo, Japan
[4]Division of Molecular Pharmacology, Cancer Chemotherapy Center, Japanese Foundation for Cancer Research, 3-8-31 Ariake, Koto-ku, 135-8550 Tokyo, Japan
[5]National Cancer Center Hospital East, 6-5-1Kashiwa, Chiba 277-8577, Japan

Human pancreatic cancer is known to be the most deadly disease with the lowest 5-year survival rate and is resistant to well known conventional chemotherapeutic drugs in clinical use. Screening of medicinal plants from Myanmar utilizing antiausterity strategy led to the identification of *Vitex negundo* as one of the medicinal plants having potent preferential cytotoxic activity against PANC-1 human pancreatic cancer cells. Bioactivity-guided phytochemical investigation led to the isolation of chrysoplenetin (1) and chrysosplenol D (2) as the active constituents with a PC_{50} value of 3.4 μg/mL and 4.6 μg/mL, respectively, against PANC-1 cells. Both these compounds induced apoptosis-like morphological changes in PANC-1 cells. Chrysoplenetin was further tested against a panel of 39 human cancer cell lines (JFCR-39) at the Japanese Foundation for Cancer Research, and 25 cell lines belonging to lung, breast, CNS, colon, melanoma, ovarian, prostate cancer and stomach cancer cell lines were found to be highly sensitive to chrysoplenetin at a submicromolar range. In the JFCR-39 panel, lung NCI-H522, ovarian OVCAR-3 and prostate PC-3 cells were found to be most sensitive with GI_{50} of 0.12, 0.18 and 0.17 μM, respectively. The COMPARE analysis suggested that the molecular mode of action of chrysoplenetin was unique compared with the existing anticancer drugs.

Keywords: PANC-1 human pancreatic cancer; *Vitex negundo*; chrysoplenetin; chrysosplenol D; JFCR-39; COMPARE.

INTRODUCTION

Cancer is the leading cause of death worldwide. An estimated 7.6 million people died of cancer in 2007 worldwide and it is projected to increase to 11.5 million deaths by 2030 (Strong *et al.*, 2008). Among the different forms of cancers, pancreatic cancer is known to be the most aggressive disease with the lowest 5-year survival rate (Li *et al.*, 2004). Almost all patients with pancreatic cancer rapidly develop metastases and die within a short period after the diagnosis (Van Cutsem *et al.*, 2009). The well known conventional chemotherapeutic agents such as taxol, doxorubicin, cisplatin and camptothecin are virtually ineffective against this cancer (Chung *et al.*, 2004). Currently, surgery is the only treatment modality that offers any prospect of potential cure. Therefore, the discovery of effective chemotherapeutic agents is urgently needed.

Human pancreatic cancer cells have inherent tolerance to extreme nutrient starvation enabling them to survive under hypovascular conditions. Therefore, agents that eliminate cancer cell tolerance to nutrition starvation are novel biochemical targets in cancer therapy (Awale *et al.*, 2006a, 2006b; Izuishi *et al.*, 2000), which are termed antiausterity agents. Working on this hypothesis, antiausterity strategy based screening of medicinal plants from wide different origins was carried out for the discovery anticancer agents with preferential cytotoxicity against PANC-1 human pancreatic cancer cells in nutrition deprived medium (NDM) (Awale *et al.*, 2006a, 2006b; Win *et al.*, 2007, 2008a, 2008b, 2008c). Recently it was observed that the methanol extract of *Vitex negundo* from Myanmar displayed potent cytotoxic activity preferentially in the nutrient starvation condition with 100% cell death at a concentration of 10 μg/mL. Therefore, it was subjected to phytochemical analysis to identify active constituents. The active constituent was further tested against PANC-1 cells as well as a panel of 39 human cancer cell lines (JFCR-39) at the Cancer Chemotherapy Center, Japanese Foundation for Cancer Research.

MATERIALS AND METHODS

Plant material. The plant materials used in this study was collected from the Pin-da-ya area, Shan state of Myanmar in September 2008. Authentication of the

* Correspondence to: Dr Shigetoshi Kadota and Dr. Suresh Awale, Institute of Natural Medicine, University of Toyama, 2630-Sugitani, Toyama 930-0194, Japan.
E-mail: kadota@inm.u-toyama.ac.jp; suresh@inm.u-toyama.ac.jp

Received 02 September 2010
Accepted 19 January 2011

plant materials was carried out by Ms Kyi Kyi Oo, Research Officer, Division of Research, University of Traditional Medicine, Mandalay, Union of Myanmar.

Extraction and isolation. Fruits of *V. negundo* (50 g) were extracted with methanol under sonication (1 L, 90 min × 3) at room temperature, and the solvent was evaporated under reduced pressure to give a MeOH extract (1.1 g). The MeOH extract was chromatographed on silica gel (19 × 4.5 cm) with a MeOH–$CHCl_3$ gradient system using MPLC to give five fractions (fr. 1: $CHCl_3$ eluate, 2.2 mg; fr. 2: 1–8% MeOH–$CHCl_3$ eluate, 246 mg; fr. 3: 9–12% MeOH–$CHCl_3$ eluate, 32.4 mg; fr. 4: 13–20% MeOH–$CHCl_3$ eluate, 75.6 mg; fr. 5: 21–30% MeOH–$CHCl_3$ eluate, 1.2 g). Fraction 2 was subjected to normal-phase preparative TLC (pTLC) with EtOAc/hexane (2:1) to afford chrysoplenetin (**1**, 30 mg). Fraction 3 was purified by reversed-phase pTLC with acetone–CH_3CN–H_2O (1:1:2) to give chrysosplenol D (**2**, 3.95 mg). Their structures were identified by spectral analysis and comparison of their data with those in the literature (Diaz *et al.*, 2003; Lai-King and Brown, 1998).

Agents. Dulbecco's modified Eagle's medium (DMEM) and Dulbecco's phosphate buffered saline (PBS) were purchased from Nissui Pharmaceutical Co., Ltd (Tokyo, Japan). The nutrient-deprived medium (NDM) was prepared following the procedure described by Izuishi *et al.* (2000). Sodium bicarbonate was purchased from Nacalai Tesque Inc. (Kyoto, Japan), and fetal bovine serum (FBS) was from Gibco BRL Products (Gaithersburg, MD, USA). Antibiotic antimycotic solution was from Sigma-Aldrich Inc. (St Louis, MO, USA). The WST-8 cell counting kit was from Dojindo (Kumamoto, Japan). The cell culture flasks and 96-well plates were from Corning Inc. (Corning, NY, USA).

Preferential cytotoxic activity of *Vitex negundo* extract against PANC-1 human pancreatic cancer cells in NDM. The *in vitro* preferential cytotoxicity of the plant extracts was determined by a previously described procedure (Awale *et al.*, 2006a). Briefly, PANC-1 human pancreatic cancer cells were seeded in 96-well plates (2×10^4/well) and incubated in fresh DMEM at 37 °C under 5% CO_2 and 95% air for 24 h. After the cells were washed with PBS, the medium was changed to either DMEM or NDM and serial dilutions of the test samples were added. After 24 h incubation, the cells were washed with PBS, and 100 µL of DMEM containing 10% WST-8 cell counting kit solution was added to the wells. After 3 h incubation, the absorbance at 450 nm was measured. The cell viability was calculated from the mean values of data from three wells by using the following equation:

$$\text{Cell viability}(\%) = \frac{Abs_{(\text{test samples})} - Abs_{(\text{blank})}}{Abs_{(\text{control})} - Abs_{(\text{blank})}} \times 100$$

Observation of morphological changes. The PANC-1 cells treated with or without the plant extract in different concentrations in NDM were incubated for 24 h. At the end of the experiment, the morphological changes of the cells were recorded by photomicrography using a phase contrast microscope (Olympus Optical Co., Ltd, Tokyo, Japan).

Evaluation of chrysoplenetin against a panel of JFCR-39 cell line. A panel of 39 human cancer cells (JFCR-39) were cultured in a previously described procedure by Yamori *et al.* (1999). The cell lines used were breast cancer (HBC-4, BSY-1, HBC-5, MCF-7, MDA-MB-231), central nervous system (CNS) cancer (U251, SF-268, SF-295, SF-539, SNB-75, SNB-78), colon cancer (HCC2998, KM-12, HT-29, HCT-15, HCT-116), lung cancer (NCI-H23, NCI-H226, NCI-H522, NCI-H460, A549, DMS273, DMS114), melanoma (LOX-IMVI), ovarian cancer (OVCAR-3, OVCAR-4, OVCAR-5, OVCAR-8, SK-OV-3), renal cancer (RXF-631 L, ACHN), prostate cancer (DU-145, PC-3) and stomach cancer (St-4, MKN1, MKN7, MKN28, MKN45, MKN74). The cells were maintained and grown in RPMI 1640 medium supplemented with 5% fetal bovine serum (FBS), penicillin (100 U/mL) and streptomycin (100 µg/mL). In brief, the cells were inoculated onto 96-well microplates and incubated for 24 h at 37 °C in humidified air containing 5% CO_2 to allow cell attachment. The medium was then replaced with the test compound at five concentrations of 10 fold dilutions, starting from a maximum of 10^{-4} M to 10^{-8} M. The cells were further incubated for 48 h, and then the cell growth was determined according to the sulforhodamine B assay method described by Rubinstein *et al.* (1990).

Data calculations were made according to the method described by Paull *et al.* (1989). The dose–response curves were plotted by the percentage of growth against $\log_{10}$ of drug concentrations and the drug concentration required for 50% growth inhibition (GI_{50}) was determined. Using the mean value, expressed as the average value of GI_{50} for chrysoplenetin against JFCR-39, a graph centered at the mean of the log GI_{50} values for all cell line responses was constructed. The projecting bars to the right or left of the mean indicated whether cell sensitivity to chrysoplenetin was more or less than average. Finally, the correlation between the mean graphs of chrysoplenetin were compared with those of the standard anticancer drugs and different types of inhibitors, using the COMPARE computer analysis developed according to the method described by Paull *et al.* (1989).

RESULTS AND DISCUSSION

Preferential cytotoxicity of *Vitex negundo* and its active constituents against PANC-1 human pancreatic cancer cells

Vitex negundo (Verbenaceae) is one of the folk medicines used widely as antipyretic, antiseptic, expectorant, menstrual disorder, to promote bone marrow function, malaria and hepatitis in Myanmar. The cytotoxic effect of the MeOH extract of *Vitex negundo* was tested against PANC-1 human pancreatic cancer cells in nutrient rich medium (DMEM) and NDM at a concentration range of 0–50 µg/mL. As shown in Fig. 1a, the extract showed preferential cytotoxicity against PANC-1 cells in NDM in a concentration-dependent manner, with 100% cell death at a concentration of 10 µg/mL in NDM. Therefore, the MeOH extract was subjected to fractionation using MPLC with silica gel to give five fractions. Each of these fractions was further

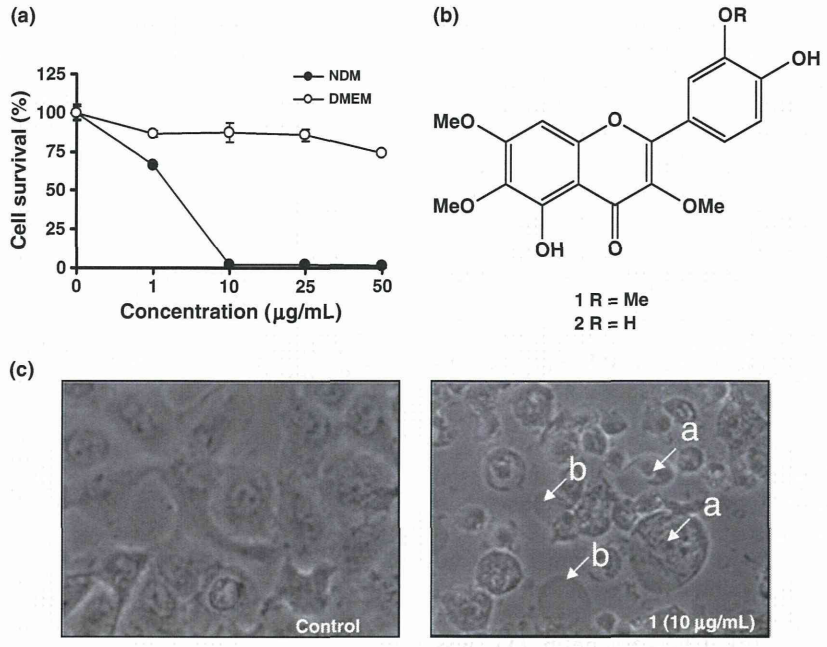

Figure 1. **(a)** Effect of the MeOH extract of *Vitex negundo* on the survival of PANC-1 human pancreatic cancer cells in DMEM and NDM. Cells were seeded at a density of 1×10^4 cells/well in a 96-well plate and incubated in DMEM and NDM in the presence of *V. negundo* extract at graded concentrations. Each point represents the mean value of triplicate experiments. **(b)** Structure of chrysoplenetin (**1**) and chrysosplenol D (**2**) isolated from the active fraction of *V. negundo*. **(c)** Effect of chrysoplenetin (**1**) on the morphology of PANC-1 human pancreatic cancer cells in NDM after 24 h exposure to 1 and 10 μg/mL. a, nucleus fragmentation and condensation; b, membrane bleb.

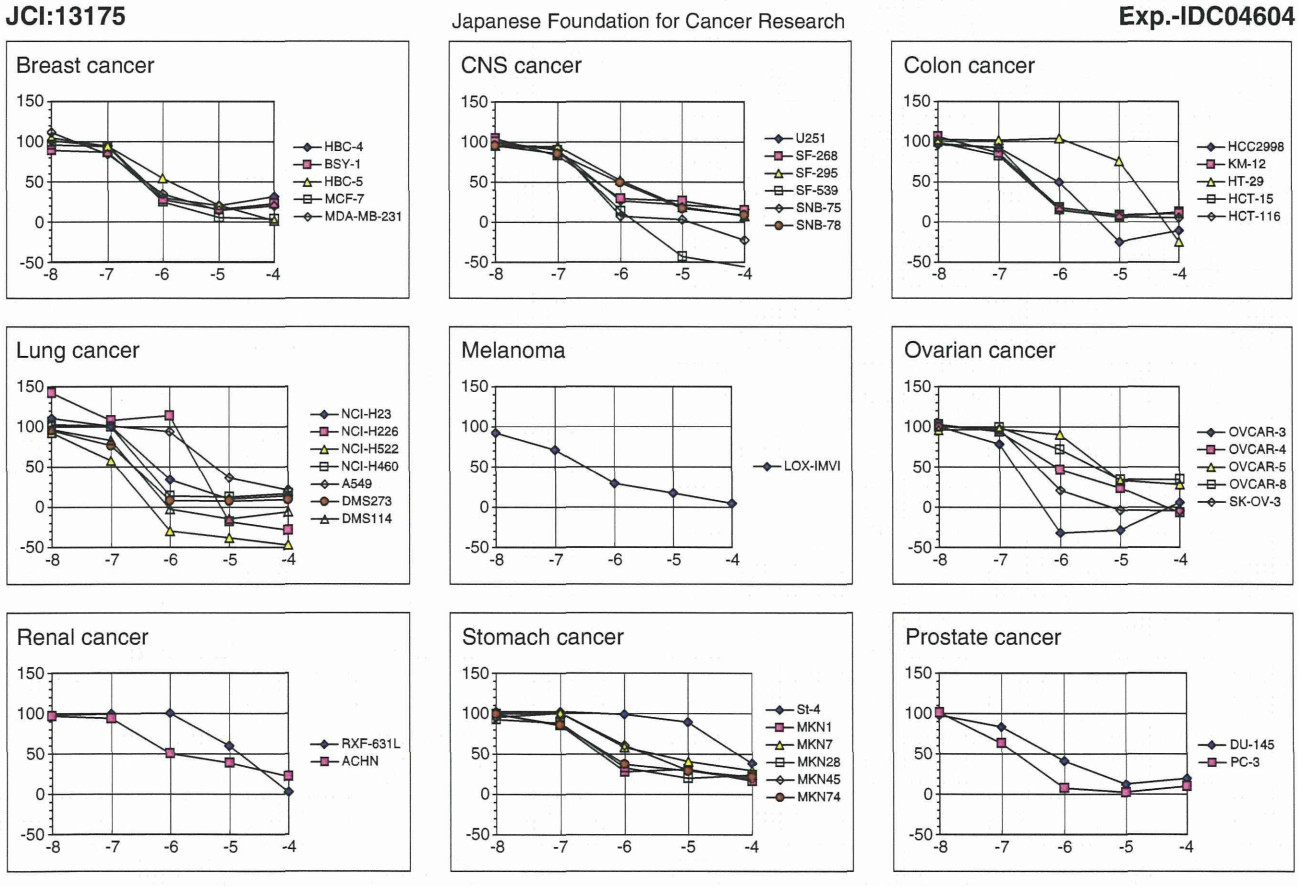

Figure 2. Dose–response curves of chrysoplenetin against the growth of JFCR-39 cells. The *x*-axis represents the concentration of chrysoplenetin and the *y*-axis represents the percentage growth. The GI_{50} represents the concentration required to inhibit cell growth by 50% compared with untreated controls.

tested for their preferential cytotoxicity. Among them fractions 1–3 showed potent activity with >90% cell death in NDM at 10 μg/mL (data not shown). Further separation of fractions 2 and 3 using preparative TLC led to the isolation of two major compounds as the active constituents responsible for the preferential cytotoxicity. The structure of these compounds (Fig. 1b) were determined based on the NMR spectroscopic analysis as chrysoplenetin (**1**) (Lai-King and Brown, 1998) and chrysosplenol D (**2**) (Diaz *et al.*, 2003).

Both of these isolated compounds were tested for their concentration-dependency in NDM. They exhibited potent preferential cytotoxicity in a concentration-dependent manner with PC_{50} value of 3.4 μg/mL (for **1**) and 4.6 μg/mL (for **2**) and showed 100% cytotoxicity at a concentration of 10 μg/mL. Arctigenin was used as a positive control in this study, displaying 100% cell death in NDM at 0.5 μg/mL. Microscopic observation of the cells treated with isolated compounds at 10 μg/mL showed clear morphological changes indicative of apoptotic cell death, such as membrane blebs, nuclear condensation and fragmentation (Fig. 1c). Chrysoplenetin (**1**) was previously reported from *Artemisia annua* (Lai-King and Brown, 1998). However, this is the first report on the occurrence of chrysoplenetin in the genus *Vitex*. On the other hand, chrysosplenol D (**2**) was reported previously from *Vitex trifolia* and *Artemisia annua* (Diaz *et al.*, 2003).

Evaluation of chrysoplenetin against a panel of 39 cancer cell lines and identification of molecular target

Chrysoplenetin, the most active compound isolated from *Vitex negundo* was further tested against a panel of 39 human cancer cell lines (JFCR-39), which includes seven lung cancer cell lines, (NCI-H23, NCI-H226, NCI-H522, NCI-H460, A549, DMS273, DMS114), five breast cancer (HBC-4, BSY-1, HBC-5, MCF-7, MDA-MB-231), six CNS cancer (U251, SF-268, SF-295, SF-539, SNB-75, SNB-78), five colon cancer (HCC2998, KM-12, HT-29, HCT-15, HCT-116), melanoma (LOX-IMVI), five ovarian cancer (OVCAR-3, OVCAR-4, OVCAR-5, OVCAR-8, SK-OV-3), two prostate cancer (DU-145, PC-3) and six stomach cancer (St-4, MKN1, MKN7, MKN28, MKN45, MKN74).

Figure 2 shows the dose–response curves of the chrysoplenetin against a panel of JFCR-39 cancer cell lines. The concentration at which the cell growth is inhibited by 50% represents GI_{50}. The GI_{50} values of chrysoplenetin against each cell line in JFCR-39 panel are shown in Table 1. Chrysoplenetin showed potent growth inhibitory activity with GI_{50} at a sub-micromolar level against 25 cancer cell lines [lung cancer cell lines (NCI-H23, NCI-H522, NCI-H460, DMS273, DMS114) breast cancer (HBC-4, HBC-5, BSY-1, MCF-7, MDA-MB-231), CNS cancer (U251, SF-268, SF-539, SNB-75), colon cancer (KM-12, HCT-15, HCT-116), melanoma (LOX-IMVI), ovarian cancer (OVCAR-3, SK-OV-3), prostate cancer (DU-145, PC-3) and stomach cancer (MKN1, MKN28, MKN74)]. Among them, lung NCI-H522, ovarian OVCAR-3 and prostate PC-3 cells were found to be the most sensitive with GI_{50} of 0.12, 0.18 and 0.17 μM, respectively. Very interestingly, chrysoplenetin showed total growth inhibition (TgI) of lung tumor cell lines NCI-H522, DMS114 at 0.46 μM and 0.95 μM, while TgI against NCI-H226, SF-539, HCC2998, SK-OV-3 was observed below 10 μM (i.e. 7.4, 1.8, 4.7 and 7.3 μM). On the other hand HT-29, St-4 and RXF-631 L showed mild activity with GI_{50} >10 μM.

Table 1. Growth inhibitory activity of chrysoplenetin against a panel of 39 human cancer cell lines (JFCR39)

Panel/Cell line	GI_{50} (μM)	TgI (μM)
Breast cancer		
HBC-4	0.49	>100
BSY-1	0.42	>100
HBC-5	1.35	>100
MCF-7	0.44	>100
MDA-MB-231	0.49	>100
CNS cancer		
U251	0.43	>100
SF-268	0.42	>100
SF-295	1.17	>100
SF-539	0.34	1.78
SNB-75	0.32	13.8
SNB-78	0.98	>100
Colon cancer		
HCC2998	1.00	4.68
KM-12	0.34	>100
HT-29	18.2	57.5
HCT-15	0.31	>100
HCT-116	0.35	>100
Lung cancer		
NCI-H23	0.58	>100
NCI-H226	3.09	7.41
NCI-H522	0.12	0.46
NCI-H460	0.38	>100
A549	5.75	>100
DMS273	0.25	>100
DMS114	0.25	0.95
Melanoma		
LOX-IMVI	0.32	>100
Ovarian cancer		
OVCAR-3	0.18	>100
OVCAR-4	0.85	60.3
OVCAR-5	5.13	>100
OVCAR-8	3.80	>100
SK-OV-3	0.42	7.24
Renal cancer		
RXF-631 L	14.8	>100
ACHN	1.15	>100
Stomach cancer		
St-4	58.9	>100
MKN1	0.41	>100
MKN7	3.02	>100
MKN28	0.49	>100
MKN45	2.19	>100
MKN74	0.55	>100
Prostate cancer		
DU-145	0.62	>100
PC-3	0.17	>100

Figure 3 shows the mean graph of logGI_{50} of each cell line produced by computer processing and represents the fingerprint of chrysoplenetin against a panel of JFCR-39 cancer cell lines. In the fingerprint, the bars extending to the right indicated sensitive cancer cell lines, while bars extending to left side indicated less sensitive cell lines. All together 24 cell lines belonging

to breast, CNS, colon, lung, melanoma and prostate cancer cell lines were found to be highly sensitive to chrysoplenetin. In the JFCR-39 panel, NCI-H522 (lung cancer) was found to be most sensitive cell line ($logGI_{50}$ −6.91), while St-4 (stomach cancer) was found to be least sensitive ($logGI_{50}$ −4.23) to chrysoplenetin. The mean $logGI_{50}$ of JFCR-39 was −6.08 (0.83 μM). The difference between the mean of $logGI_{50}$ of the most sensitive cell line (δ value) and the difference between the $logGI_{50}$ of the most resistant cell line and the $logGI_{50}$ of the most sensitive one (range value) were 0.83 and 2.68, respectively, which satisfied both δ (≥0.5) and range (≥1) values for a positive evaluation of an anticancer candidate in the JCI protocol. The selectivity between the most sensitive line (NCI-H522, log GI_{50} −6.91) and the least sensitive line (St-4, $logGI_{50}$ −4.23) was more than 500 fold. Within the same cancer subpanel, a selectivity of >100 fold was observed between St-4 and MKN1 (stomach cancer) and >50 fold between HCT-15 and HT-29 (colon cancer), respectively.

The JFCR-39 panel is a powerful tool for drug evaluation because it is combined with a database of drug sensitivities of standard compounds including various anticancer drugs and inhibitors of biological pathways (>700 compounds) (Dan *et al.*, 2002, 2010; Yamori *et al.*, 1999). The COMPARE analysis (Nakatsu *et al.*, 2007; Yaguchi *et al.*, 2006) predicts a possible mode of action or a molecular target of the testing compound based on the similarity of the mean graphs between the testing and standard compounds. Using COMPARE analysis in the present study, vincristine, a tubulin polymerization inhibitor, was identified as the drug most similar to chrysoplenetin. However, the correlation coefficient was marginal ($r = 0.536$). Therefore, it was rather suggested that the molecular mode of action of chrysoplenetin, was unique compared with the existing anticancer drugs.

In summary, the ethanol extract of *V. negundo* showed potent preferential cytotoxicity against PANC-1 human pancreatic cancer cells. Bioassay-guided fractionation and purification of *Vitex negundo* led to the isolation of chrysoplenetin (**1**) and chrysosplenol D (**2**) as the most active constituents with a PC_{50} value of 3.4 μg/mL and 4.6 μg/mL, respectively, against the PANC-1 human pancreatic cancer cell line. They showed characteristic apoptosis-like morphological changes of PANC-1 cells in NDM. The most active compound, chrysoplenetin was further evaluated against a panel of 39 human cancer cell lines at the Japanese Foundation for Cancer Research. Chrysoplenetin exhibited differential cell growth inhibition at submicromolar concentration against most of the cell lines. *Vitex negundo* and its active

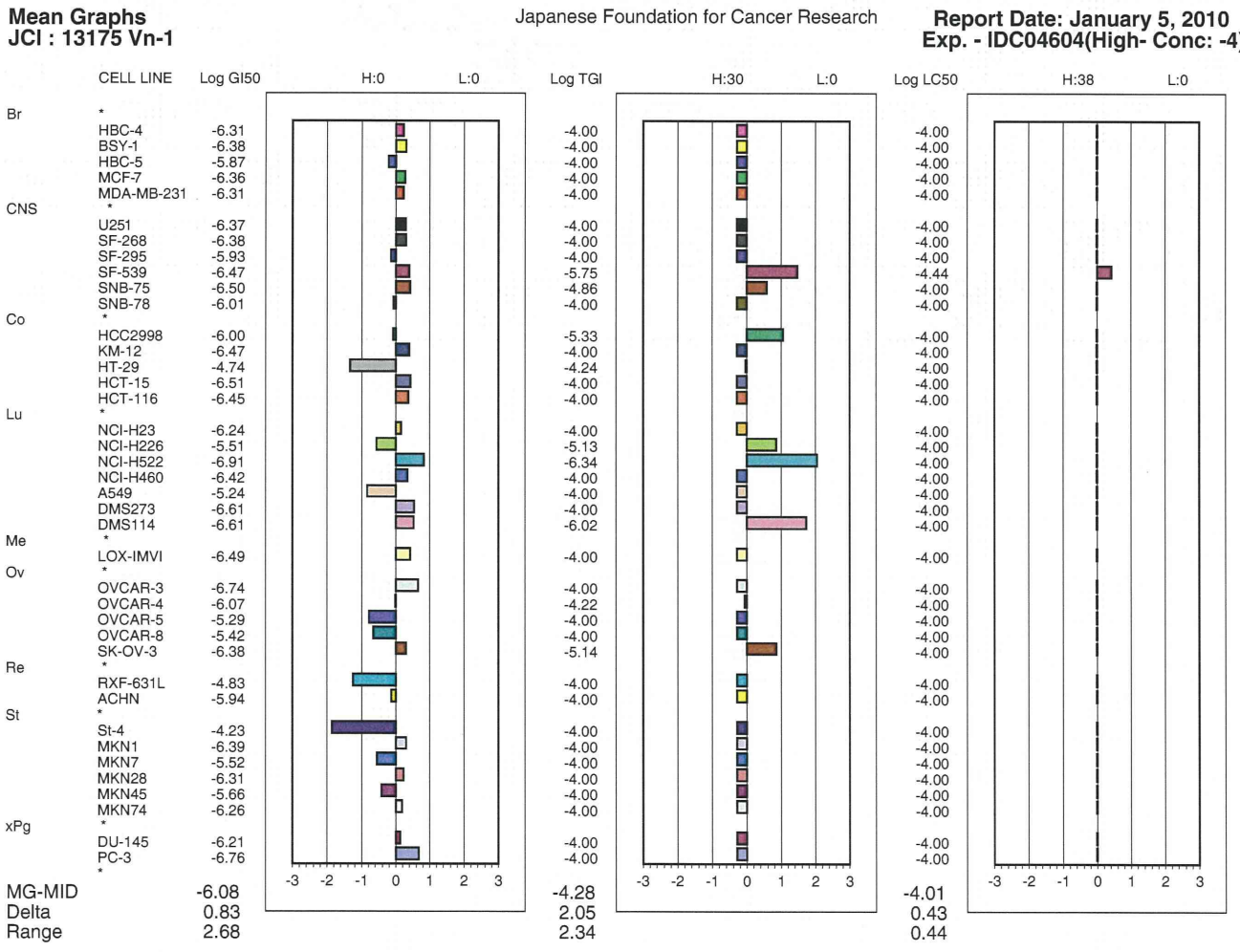

Figure 3. Fingerprint of chrysoplenetin showing the differential growth inhibition pattern of the cells in the JFCR-39 cells. The *x*-axis represents the relative value of GI_{50}; (−1) × (log GI_{50} − MG-MID); MG-MID is the mean value of the log GI_{50}. Exp-ID and JCI numbers are the ID for the experiment and ID for the chrysoplenetin, respectively, in the database of JFCR.

constituents might have possible beneficial effects for patients suffering from cancer in a real clinical situation.

Acknowledgement

This work was supported by a grant from the Ministry of Health and Welfare for the Third-Term Comprehensive 10-Year Strategy for Cancer Control. One of the authors (T. Z. L.) acknowledges JSPS ROMPAKU program, Ministry of Education, Culture, Sports, Science and Technology, Japan.

Conflict of Interest

The authors have declared that there is no conflict of interest.

REFERENCES

Awale S, Lu J, Kalauni SK *et al.* 2006a. Identification of arctigenin as an antitumor agent having the ability to eliminate the tolerance of cancer cells to nutrient starvation. *Cancer Res* **66**: 1751–1757.

Awale S, Nakashima EMN, Kalauni SK *et al.* 2006b. Angelmarin, a novel anti-cancer agent able to eliminate the tolerance of cancer cells to nutrient starvation. *Bioorg Med Chem Lett* **16**: 581–583.

Chung HW, Bang SM, Park SW *et al.* 2004. A prospective randomized study of gemcitabine with doxifluridine versus paclitaxel with doxifluridine in concurrent chemoradiotherapy for locally advanced pancreatic cancer. *Int J Radiat Oncol Biol Phys* **60**: 1494–1501.

Dan S, Okamura M, Seki M *et al.* 2010. Correlating phosphatidylinositol 3-kinase inhibitor efficacy with signaling pathway status: in silico and biological evaluations. *Cancer Res* **70**: 4982–4994.

Dan S, Tsunoda T, Kitahara O *et al.* 2002. An integrated database of chemosensitivity to 55 anticancer drugs and gene expression profiles of 39 human cancer cell lines. *Cancer Res* **62**: 1139–1147.

Diaz F, Chavez D, Lee D *et al.* 2003. Cytotoxic flavone analogues of vitexicarpin, a constituent of the leaves of *Vitex negundo*. *J Nat Prod* **66**: 865–867.

Izuishi K, Kato K, Ogura T, Kinoshita T, Esumi H. 2000. Remarkable tolerance of tumor cells to nutrient deprivation: possible new biochemical target for cancer therapy. *Cancer Res* **60**: 6201–6207.

Lai-King S, Brown GD. 1998. Three sesquiterpenes from *Artemisia annua*. *Phytochemistry* **48**: 1207–1211.

Li D, Xie K, Wolff R, Abbruzzese JL. 2004. Pancreatic cancer. *Lancet* **363**: 1049–1057.

Nakatsu N, Nakamura T, Yamazaki K *et al.* 2007. Evaluation of action mechanisms of toxic chemicals using JFCR39, a panel of human cancer cell lines. *Mol Pharmacol* **72**: 1171–1180.

Paull KD, Shoemaker RH, Hodes L *et al.* 1989. Display and analysis of patterns of differential activity of drugs against human tumor cell lines: development of mean graph and COMPARE algorithm. *J Nat Cancer Inst* **81**: 1088–1092.

Rubinstein LV, Shoemaker RH, Paull KD *et al.* 1990. Comparison of *in vitro* anticancer-drug-screening data generated with a tetrazolium assay versus a protein assay against a diverse panel of human tumor cell lines. *J Nat Cancer Inst* **82**: 1113–1118.

Strong K, Mathers C, Epping-Jordan J, Resnikoff S, Ullrich A. 2008. Preventing cancer through tobacco and infection control: how many lives can we save in the next 10 years? *Eur J Cancer Prev* **17**: 153–161.

Van Cutsem E, Vervenne WL, Bennouna J *et al.* 2009. Phase III Trial of Bevacizumab in combination with gemcitabine and erlotinib in patients with metastatic pancreatic cancer. *J Clin Oncol* **27**: 2231–2237.

Win NN, Awale S, Esumi H, Tezuka Y, Kadota S. 2007. Bioactive secondary metabolites from *Boesenbergia pandurata* of Myanmar and their preferential cytotoxicity against human pancreatic cancer PANC-1 cell line in nutrient-deprived medium. *J Nat Prod* **70**: 1582–1587.

Win NN, Awale S, Esumi H, Tezuka Y, Kadota S. 2008a. Novel anticancer agents, kayeassamins A and B from the flower of *Kayea assamica* of Myanmar. *Bioorg Med Chem Lett* **18**: 4688–4691.

Win NN, Awale S, Esumi H, Tezuka Y, Kadota S. 2008b. Novel anticancer agents, kayeassamins C-I from the flower of Kayea assamica of Myanmar. *Bioorg Med Chem* **16**: 8653–8660.

Win NN, Awale S, Esumi H, Tezuka Y, Kadota S. 2008c. Panduratins D–I, novel secondary metabolites from rhizomes of *Boesenbergia pandurata*. *Chem Pharm Bull* **56**: 491–496.

Yaguchi S-I, Fukui Y, Koshimizu I *et al.* 2006. Antitumor activity of ZSTK474, a new phosphatidylinositol 3-kinase inhibitor. *J Natl Cancer Inst* **98**: 545–556.

Yamori T, Matsunaga A, Sato S *et al.* 1999. Potent antitumor activity of MS-247, a novel DNA minor groove binder, evaluated by an *in vitro* and *in vivo* human cancer cell line panel. *Cancer Res* **59**: 4042–4049.

Cancer Science
The official journal of the Japanese Cancer Association

Hypoglycemic/hypoxic condition *in vitro* mimicking the tumor microenvironment markedly reduced the efficacy of anticancer drugs

Hiroko Onozuka,[1,2] Katsuya Tsuchihara[1] and Hiroyasu Esumi[1,2,3]

[1]Cancer Physiology Project, Research Center for Innovative Oncology, National Cancer Center Hospital East, Kashiwa, Chiba; [2]Department of Integrated Biosciences, Graduate School of Frontier Sciences, The University of Tokyo, Kashiwa, Chiba, Japan

(Received November 23, 2010/Revised January 14, 2011/Accepted January 18, 2011/Accepted manuscript online January 21, 2011/Article first published online March 7, 2011)

Tumor tissues are often hypoxic because of defective vasculature. We previously showed that tumor tissues are also often deprived of glucose. The efficacy of anticancer drugs is affected by the tumor microenvironment, partly because of the drug delivery and cellular drug resistance; however, the precise mechanisms remain to be clarified. In the present study, we attempted to clarify whether hypoglycemic/hypoxic condition, which mimics the tumor microenvironment, might induce drug resistance, and if it did, to elucidate the underlying mechanisms. Pancreatic cancer-derived PANC-1 cells were treated with serial dilutions of anticancer drugs and incubated in either normoglycemic (1.0 g/L glucose) or hypoglycemic (0 g/L glucose) and normoxic (21% O_2) or hypoxic (1% O_2) conditions. The 50% inhibitory concentration of gemcitabine was 1000 times higher for PANC-1 cells incubated under the hypoglycemic/hypoxic condition than for those incubated under the normoglycemic/normoxic condition. Conventional anticancer drugs target rapidly growing cells, so that non-proliferating or slowly proliferating cells usually show resistance to drugs. Though the cell cycle was delayed, sufficient cellular uptake and DNA incorporation of gemcitabine occurred under the hypoglycemic/hypoxic condition to cause DNA lesions and S-phase arrest. To overcome hypoglycemic/hypoxia-induced drug resistance, we examined kinase inhibitors targeting Chk1 or cell-survival signaling pathways. Among the compounds examined, the combination of UCN-01 and LY294002 partially sensitized the cells to gemcitabine under the hypoglycemic/hypoxic condition. These findings suggested that the adoption of suitable strategies may enhance the cytotoxicities of clinically used anticancer drugs against cancer cells. (*Cancer Sci* 2011; 102: 975–982)

It is widely accepted that solid tumors are heterogeneous in structure as a result of unregulated cancer cell proliferation, presence of several cell types and aberrant vessel formation. Among these, the tumor vasculature has a major impact on the tumor microenvironment. In normal tissue, vascular networks generally develop in a well-ordered hierarchal fashion, so that an insufficient blood supply seldom occurs. In contrast, tumor vascular networks undergo continuous remodeling, because unregulated cell proliferation destroys the existing tissue structures. Previous structural analyses had clearly shown that tumors exhibit aberrant and poorly organized vasculature without any hierarchy.[1–4]

As a consequence of the poorly organized vasculature in tumors, the delivery of oxygen is extremely limited. Direct measurement of the oxygen tension in cancer tissues has demonstrated the presence of severely hypoxic regions in many types of cancers.[5] Although hypoxia is also toxic to cancer cells, cancer cells adapt through genetic and epigenetic changes that allow them to survive and even proliferate in hypoxic environments.[6–9] Hypoxia-inducible factor-1α (HIF-1α) is a key transcription factor for downstream hypoxia-inducible genes, which regulate several biological processes in hypoxic environments.[10–12] Hypoxia response pathways overlap with many of the known oncogenic signaling pathways and also contribute to tumor aggressiveness.[13–15] Therefore, tumor hypoxia is regarded as a good target for cancer therapy. Meanwhile, cancer cells predominantly use the glycolytic pathway, rather than oxidative phosphorylation, for energy production, irrespective of the oxygen availability (Warburg effect).[16,17] In addition to the intrinsic predisposition of cancer cells to metabolize glucose, HIF-1α has been shown to regulate the expressions of all the enzymes involved in the glycolytic pathway, which mediate cellular glucose uptake.[18,19] The activation of HIF-1α enables cancer cells to use excessive glucose to maintain cellular homeostasis in hypoxic environments, causing depletion of glucose from the surrounding tissues. Indeed, a metabolomic analysis of stomach and colon cancer tissues has clearly showed glucose depletion in the tumor tissues as compared to normal tissues, indicating that several regions of tumor tissues are characterized by both hypoxia and hypoglycemia.[20] However, little is known about the biology of cancer cells under hypoglycemic condition.

Although many molecular-targeting drugs have been introduced for clinical use, conventional anticancer drugs are in wide clinical use and continue to confer many clinical benefits. Heterogeneity in the tumor microenvironment provides cancer cells the opportunity to escape from anticancer drugs. One of the processes affected by the heterogeneity of tumors is drug diffusion.[21,22] In addition, many types of drug resistance of the cells to anticancer drugs are known to occur, and overexpression of the ABC transporter is a representative mechanism.[23–25] Recent studies have reported that drug resistance may also be related to the tumor microenvironment, especially hypoxia, and the clinical relevance of such resistance. Three-dimensional culture system is used as a useful new strategy to represent tumor microenvironment *in vitro*.[26,27] However, the detailed molecular mechanisms for the resistance are largely unclear. In this study, we clarified how hypoglycemic/hypoxic condition might affect the efficacies of anticancer drugs.

Materials and Methods

Cell lines and culture conditions. The human pancreatic ductal adenocarcinoma cell lines PANC-1 and Capan-1 and the hepatoma-derived cell line HepG2 were purchased from ATCC (American Type Culture Collection, Rockville, MD, USA). PSN-1 was gifted from the Genetics Division of the National Cancer Center Research Institute (Tokyo, Japan). All cell lines were maintained in DMEM (Nissui, Tokyo, Japan). A

[3]To whom correspondence should be addressed. E-mail: hesumi@east.ncc.go.jp

doi: 10.1111/j.1349-7006.2011.01880.x

glucose-deprived condition was achieved by culturing the cells in glucose-free medium (Sigma, St. Louis, MO, USA). A hypoxic condition was achieved by incubating the cells in a hypoxia incubator in the presence 5% CO_2 and 1% O_2. The experiments were performed using PANC-1 cells, unless stated otherwise.

Reagents. Gemcitabine (Gemzar; Eli Lilly Co., Indianapolis, IN, USA) and 5-fluorouracil (Kyowa Hakko Kirin Co., Ltd, Tokyo, Japan) were dissolved in saline and stored at −20°C. Cisplatin (Sigma) was dissolved in DMSO on the day of use. UCN-01 was kindly provided by Kyowa Hakko Kirin Co., Ltd. LY294002 and Gö6976 were purchased from Calbiochem (San Diego, CA, USA). Antibodies were purchased from the following manufacturers: anti-total Akt, anti-phosphospecific Akt (Ser 473), anti-phosphospecific Cdc25c (Ser216), anti-phosphor specific Chk1 (Ser345), anti-phosphospecific Chk2 (Thr68), and anti-γ-H2AX (Ser139) from Cell Signaling Technology (Danvers, MA, USA); anti-HIF-1α and anti-HIF-2α antibodies from Novus Biologicals (Littleton, CO, USA); Chk1 (G-4) and Actin (C-11) antibodies from Santa Cruz Biotechnology (Santa Cruz, CA, USA); Chk2 antibody clone7 from Upstate Biotechnology (Lake Placid, NY, USA). The following secondary antibodies were purchased from Santa Cruz Biotechnology: goat antimouse IgG-HRP, goat antirabbit IgG-HRP, and donkey antigoat IgG-HRP.

Cytotoxicity assay of anticancer drugs. The cytotoxicity assay was performed using Cell Counting kit-8 (Dojindo Molecular Technologies, Kumamoto, Japan), as described previously.[28] The cell number in the absence of anticancer drugs under each culture condition was set as 100%. Values shown represent the means ± SD (n = 4–8).

siRNA transfection. SMARTpool HIF-1α, HIF-2α, Chk1, Chk2 and non-silencing siRNA were purchased from Dharmacon (Lafayette, CO, USA). Cells were seeded at 10^6 cells per dish in 10 mm dishes. At 24 h after seeding, siRNA was added at a final concentration of 100 nM, followed by incubation for 24 h. The knockdown efficacies were determined by Western blot analysis.

Western blot analysis. Protein extraction and Western blot analysis were performed as described previously.[29] The antibody dilutions used were in accordance with the manufacturers' instructions.

Cell cycle analysis. After 24 h preincubation, 1×10^6 cells were cultured in a 60-mm cell culture dish under either normoglycemic/normoxic or hypoglycemic/hypoxic conditions for 24 h, followed by staining using the Click-iT EdU Alexa Fluor 488 Cell Proliferation Assay kit (Molecular Probes, Eugene, OR, USA) in accordance with the manufacturer's instructions, and analyzed on a FACSCalibur (BD Bioscience, San Jose, CA, USA).

DNA ploidy assay. After 24 h preincubation, 1×10^6 cells were cultured in a 60-mm cell culture dish under either normoglycemic/normoxic or hypoglycemic/hypoxic conditions in the presence or absence of 1 μM gemcitabine for 24 h, followed by staining with propidium iodide (Molecular Probes) in accordance with the manufacturer's instruction, and analyzed on a FACSCalibur.

[^{3}H]-Gemcitabine and [^{3}H]-thymidine uptake. After 24 h preincubation, 1×10^6 cells were cultured in a 60-mm cell culture dish under either normoglycemic/normoxic or hypoglycemic/hypoxic conditions for 24 h, followed by incubation for another 3 h with 1 μM [^{3}H]-labeled gemcitabine (6.8 μCi/nmol; Moravek Biochemicals, Brea, CA, USA). The cells were washed thrice with complete medium containing 100 μM gemcitabine, and twice with ice-cold PBS. The cells were detached by trypsinization and counted by the Trypan blue exclusion method. The total cellular uptake of [^{3}H]-gemcitabine was measured by lysing a 10 μL aliquot of the cell suspension and counting the total cell-associated radioactivity using a multipurpose scintillation counter, LS6500 (Beckman Coulter Inc., Fullerton, CA, USA). The incorporation of [^{3}H]-gemcitabine into the DNA was determined by a previously published method, with slight modification.[30]

Statistical analysis. All the results were expressed as the mean ± SD. The statistical analysis was conducted using the Student t-test after an ANOVA.

Results

Effect of the culture condition on the sensitivity to various anticancer drugs. In the first set of experiments, we determined whether hypoxia and hypoglycemia might affect the sensitivity of the cancer cells to gemcitabine, 5-fluorouracil and cisplatin, which are commonly used drugs for systemic chemotherapy of cancer. Pancreatic cancer-derived PANC-1 cells were treated with serial dilutions of anticancer drugs and incubated under either a normoglycemic (1.0 g/L glucose) or hypoglycemic (0 g/L glucose) condition and normoxic (21% O_2) or hypoxic (1% O_2) condition. The 50% inhibitory concentration (IC_{50}) of gemcitabine for the PANC-1 cells incubated under the normoglycemic/normoxic condition was 300 nM, whereas the IC_{50} values of gemcitabine under the hypoxic and hypoglycemic condition were >300 μM, which was 1000 times higher than the value under the normoglycemic/normoxic condition (Fig. 1A). Similarly, the IC_{50} of 5-fluorouracil was greatly influenced by the culture condition, with IC_{50} values of 2.7 μM under the normoglycemic/normoxic condition, 9.6 μM under the hypoglycemic/normoxic condition, 92 μM under the normoglycemic/hypoxic condition, and 79 μM under the hypoglycemic/hypoxic condition (Fig. 1B); the corresponding values for cisplatin were 74, 106, 108 μM, and more than 300 μM (Fig. 1C). The cytotoxicities of gemcitabine for other pancreatic cancer cell lines, PSN-1 and Capan-1, were also examined. The IC_{50} of gemcitabine for the PSN-1 cells was 0.22 μM under the normoglycemic/normoxic condition and more than 300 μM under the hypoglycemic/hypoxic condition (Fig. 1D). The IC_{50} of gemcitabine for the Capan-1 cells was 0.24 μM under the normoglycemic/normoxic condition, and 57 μM under the hypoglycemic/hypoxic condition (Fig. 1E). The sensitivities of the hepatoma-derived HepG2 cells, which express wild-type p53, were also examined. The IC_{50} of gemcitabine for HepG2 cells was 2.9 μM under the normoglycemic/normoxic condition, and more than 300 μM under the hypoglycemic/hypoxic condition (Fig. 1F).

Cell-cycle progression and gemcitabine uptake under various culture conditions. During cell proliferation, cells must prepare to double all their components. The restriction of nutrient and oxygen supply might greatly influence the cell-cycle progression, through complex mechanisms.[31] Gemcitabine is incorporated into the DNA to exert its cytotoxicity.[32,33] Therefore, the cell-cycle analysis was conducted under the hypoglycemic/hypoxic condition. Newly synthesized DNA was labeled with 5-ethynil-2′-deoxyuridine (EdU), and the DNA content was labeled with 7-aminoactinomycin D, followed by multicolor analysis by flow-cytometry. About 45% of the cells under the normoglycemic/normoxic condition and 41% of the cells under the hypoglycemic/hypoxic condition were in the S-phase. Thus, the S-phase population was almost the same under both conditions. Closer analysis of the S-phase populations under both conditions indicated that the numbers of cells in the late S and G2 phases were reduced under the hypoglycemic/hypoxic condition, indicating S-phase prolongation (Fig. 2A). The cellular uptake and DNA incorporation of gemcitabine were directly assessed using [^{3}H]-labeled gemcitabine. Cells were cultured under the normoglycemic/normoxic or hypoglycemic/hypoxic condition for 24 h, followed by incubation with 1 μM [^{3}H]-gemcitabine for 3 h. The cellular uptake of gemcitabine was almost

doi: 10.1111/j.1349-7006.2011.01880.x

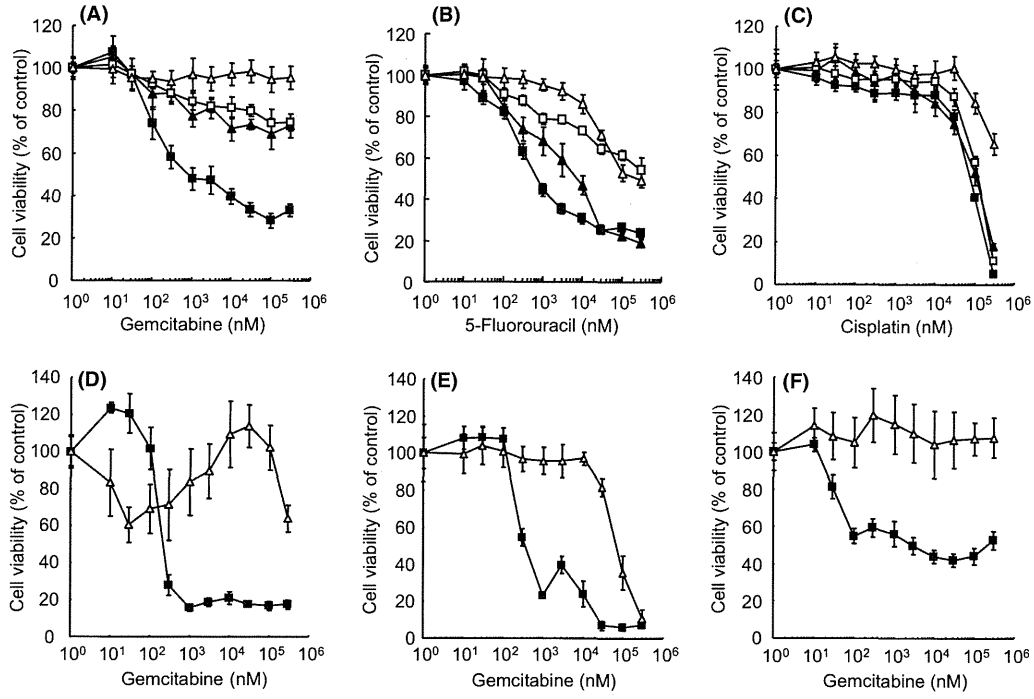

Fig. 1. Effect of the culture condition on the cytotoxicity of anticancer drugs. The cytotoxicity of (A) gemcitabine, (B) 5-fluorouracil and (C) cisplatin on the PANC-1 cells was examined. Cytotoxicity of gemcitabine on (D) the Capan-1, (E) PSN-1 and (F) HepG2 cells were also examined. (■) normoglycemic/normoxic, (▲) hypoglycemic/normoxic, (□) normoglycemic/hypoxic, and (△) hypoglycemic/hypoxic conditions.

twofold higher and the DNA incorporation of [^{3}H]-gemcitabine was almost fivefold higher under the hypoglycemic/hypoxic condition than under the normoglycemic/normoxic condition (Fig. 2B).

Gemcitabine-induced checkpoint activation and S-phase arrest. DNA incorporation of gemcitabine cause the replication fork to stall; this, in turn, induces S-phase checkpoint activation and S-phase arrest or apoptosis.[34,35] To analyze the signaling by gemcitabine-induced DNA lesions, we examined checkpoint kinase activations. After 12 h incubation in the presence or absence of 1 and 100 μM gemcitabine, phosphorylation of H2AX, Chk1 and Chk2 were induced by gemcitabine equally under different culture conditions (Fig. 2C). We further examined gemcitabine-induced S-phase arrest using propidium iodide staining and flow-cytometric analysis. S-phase arrest was equally induced by gemcitabine under the normoglycemic/normoxic and hypoglycemic/hypoxic conditions (Fig. 2D).

Effect of inhibition of Chk1 signaling on the cytotoxicity of gemcitabine. Previous studies have shown that UCN-01 and Gö6976 sensitized cells to gemcitabine via Chk1 inhibition, resulting in abrogation of the cell cycle arrest and subsequent cell death.[36–39] We examined the sensitivity of Chk1 signaling-inhibited cells to gemcitabine under the hypoglycemic/hypoxic condition. Western blot analysis showed that 1 μM of the Chk1 inhibitors, UCN-01 and Gö6976, reduced the phosphorylation of cdc25c, a downstream mediator of Chk1 (Fig. 3A); UCN-01 and Gö6976 lowered the IC_{50} of gemcitabine by more than 10 times under the normoglycemic/normoxic condition, but not under the hypoglycemic/hypoxic condition (Fig. 3B,C). Similar results were obtained with 10 μM UCN-01 or Gö6976. To confirm these results, the effect of an RNAi for Chk1 was examined. The RNAi effectively suppressed Chk1 activation under both the normoglycemic/normoxic and hypoglycemic/hypoxic conditions (Fig. 3D); however, Chk1 suppression enhanced the sensitivity of the cells to gemcitabine only under the normoglycemic/normoxic condition (Fig. 3E).

Effect of inhibition of the HIFs and PI3K/Akt signaling on the sensitivity of the cancer cells to gemcitabine. HIF-1α is induced by hypoxia and modifies cell survival.[40,41] Under the hypoxic condition, the HIF-1α protein levels increased rapidly to peak within 2 h and thereafter decreased (Fig. 4A). The HIF-2α protein level was also rapidly induced within 2 h, and maintained for 24 h. The HIF-1α protein level decreased, but not the HIF-2α protein levels, under the hypoglycemic condition (Fig. 4A). To evaluate the involvement of the HIFs in the resistance to gemcitabine, HIF-1α or HIF-2α expression was suppressed by RNAi and the sensitivity of the cells to gemcitabine was examined. RNAi for HIF-1α and HIF-2α effectively suppressed the hypoxia-induced accumulation of the respective proteins (Fig. 4B). Knockdown of HIF-1α, HIF-2α or HIF-1/2α did not have any effect on the sensitivity of the cells to gemcitabine under hypoxic condition (Fig. 4C–E). Akt is known to be activated by hypoglycemic condition and to play some roles in cell survival.[42,43] In our study, marked increase of Akt phosphorylation at ser473 was observed within 2 h under both the hypoglycemic and hypoxic condition, which was sustained for at least 24 h; the increase was, however, more evident under the hypoxic condition (Fig. 4A). To examine the involvement of PI3K/Akt signaling in the drug resistance, we utilized a PI3K inhibitor, LY294002. After treatment with LY294002 (10 and 20 μM) for 24 h, Akt phosphorylation was effectively inhibited to less than the basal level (Fig. 4F). Although treatment with 20 μM of LY294002 reduced the IC_{50} of gemcitabine by 15-fold under the normoglycemic/normoxic condition, it had little effect under the hypoglycemic/normoxic condition (Fig. 4G).

Effect of combined inhibition of Chk1 and HIF signaling on the drug resistance induced by hypoglycemic/hypoxic condition. Inhibition of either checkpoint to produce release from the gemcitabine-induced S-phase arrest or of cell-survival signaling under hypoxia, HIFs, and under hypoglycemia Akt, each alone was not effective to ameliorate the resistance to gemcitabine. We examined the combined inhibition of Chk1 and

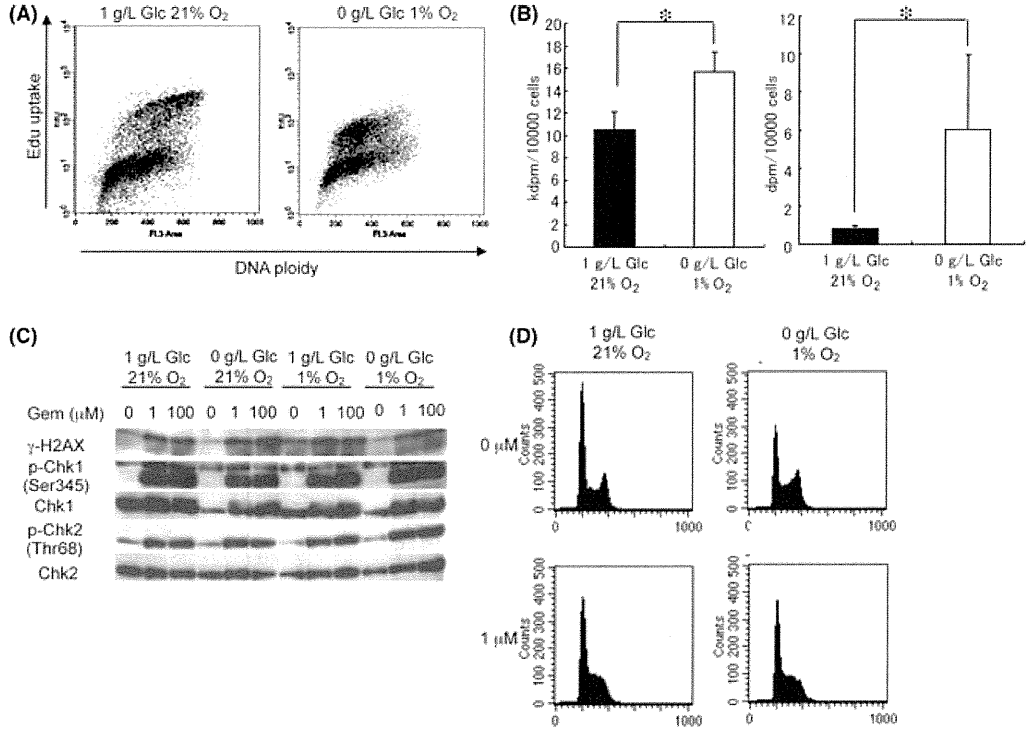

Fig. 2. Cell-cycle progression, uptake of gemcitabine and gemcitabine-induced cellular responses under various conditions. (A) Representative cell-cycle distribution detected by EdU incorporation and flow cytometry. Three independent experiments were carried out. (B) Cellular uptake and DNA incorporation of [^{3}H] gemcitabine (*$P < 0.05$). (C) Phosphorylations of H2AX, Chk1 and Chk2 detected by Western blot analysis after 12 h treatment with the indicated concentration of gemcitabine. (D) Representative DNA ploidy patterns after 24 h treatment with 1 μM gemcitabine. Three independent experiments were carried out.

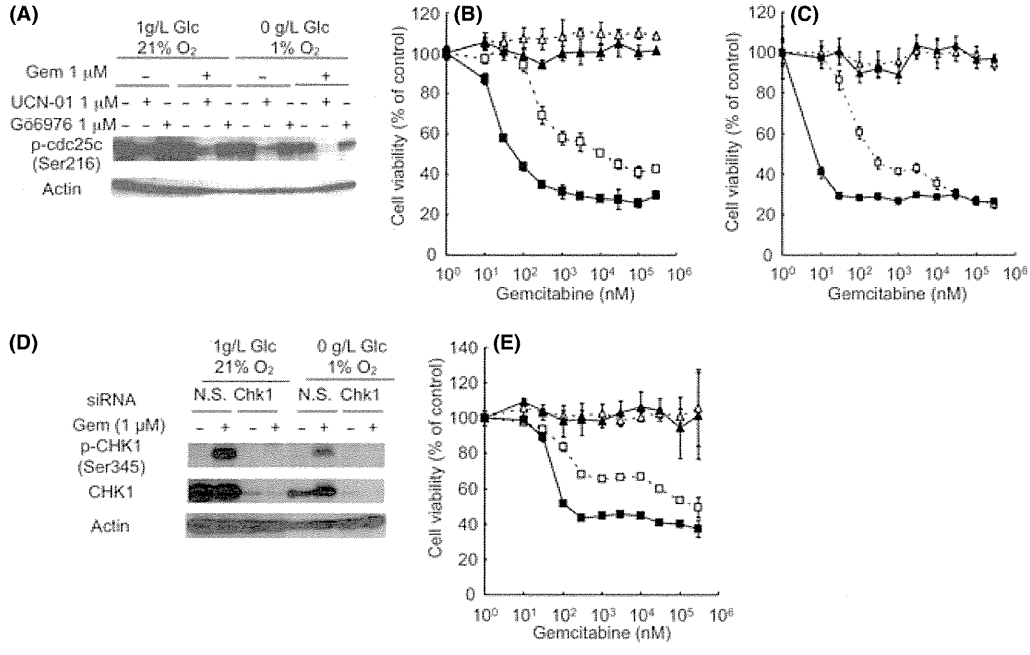

Fig. 3. Effect of inhibition of Chk1 signaling on the sensitivity of cells to gemcitabine. (A) Western blot analysis of cdc25c in the presence of Chk1 inhibitors under the indicated conditions. Cytotoxicity of gemcitabine in the presence or absence of 1 μM (B) UCN-01, (C) or Gö6976 under (■ or □) normoglycemic/normoxic condition or (▲ or △) hypoglycemic/normoxic condition. (D) Western blot analysis of Chk1 expression and activation. (E) The cytotoxicity of gemcitabine with or without Chk1 knockdown under (□ or ■) normoglycemic/normoxic condition or (△ or ▲) hypoglycemic/hypoxic condition.

doi: 10.1111/j.1349-7006.2011.01880.x

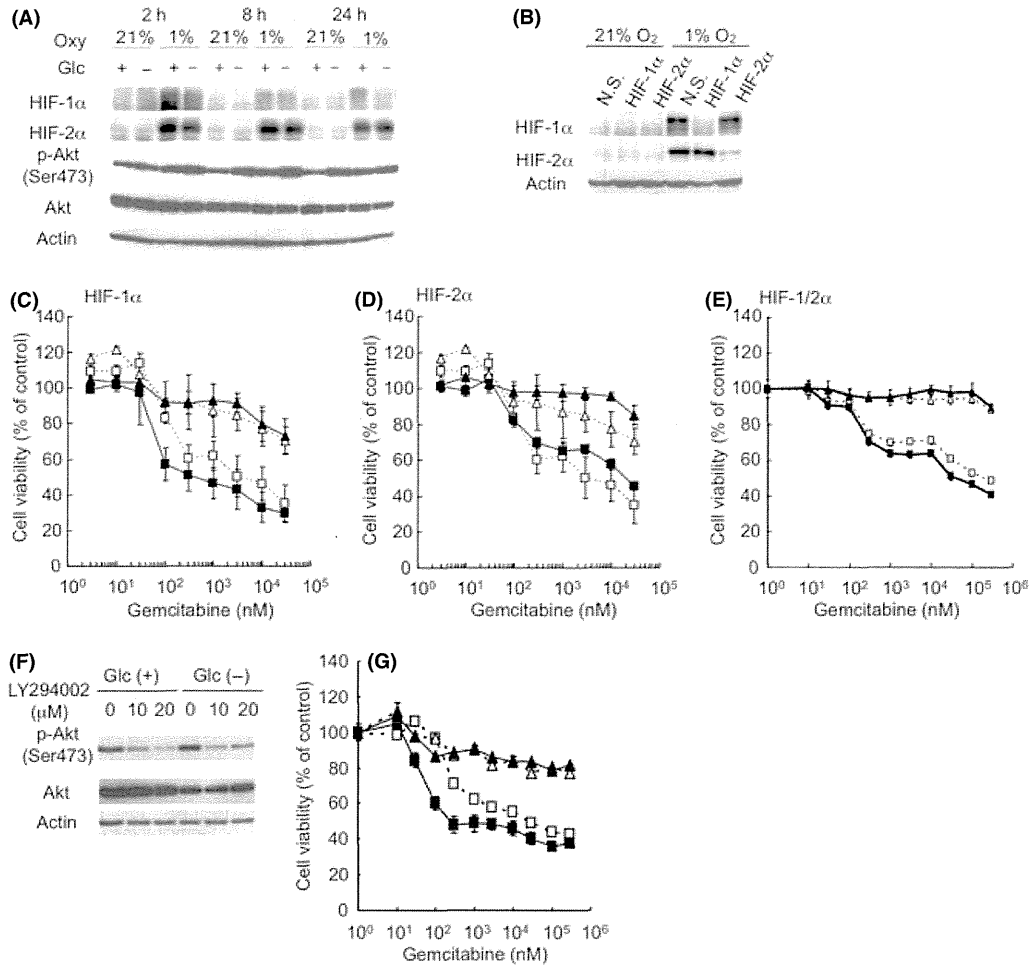

Fig. 4. Effects of inhibition of HIFs and PI3K/Akt signaling on the sensitivity of the cells to gemcitabine. (A) Western blot analysis for HIF1α and 2α accumulation and Akt phosphorylation under the indicated oxygen tension, normoxia (21%), or hypoxia (1%), and in the presence of a glucose concentration of 1 g/L (+) or 0 g/L (−). (B) Western blot analysis for HIF1α and 2α protein in cells treated with HIF-1α or HIF-2α siRNA. The cytotoxicity of gemcitabine on (C) HIF-1α, (D) HIF-2α or (E) HIF-1/2α knockdown cells or control cells under (■ or □) normoglycemic/normoxic condition or (▲ or △) normoglycemic/hypoxic condition. (F) Phosphorylation of Akt in the presence of 10 or 20 μM LY294002 under the indicated culture conditions. (G) Cytotoxicity of gemcitabine in the presence or absence of 20 μM LY294002 under (■ or □) normoglycemic/normoxic condition or (▲ or △) hypoglycemic/normoxic condition.

HIF signaling: HIF-1α, HIF-2α, or HIF-1/2α knockdown cells were examined for their sensitivity to gemcitabine in the presence of 1 μM UCN-01; however, even such combined inhibition was found to have no effect on the sensitivity of the cells to gemcitabine under the hypoxic condition (Fig. 5).

Effect of combined inhibition of Chk1 and PI3K signaling on the drug resistance induced by hypoglycemic/hypoxic condition. Combined inhibition of Chk1 and PI3K signaling was examined. As shown in Figure 6 1μM UCN-01 and 20 μM LY294002 strongly enhanced gemcitabine cytotoxicity under both normoglycemic/normoxic and hypoglycemic/hypoxic conditions, although the effect under the hypoglycemic/hypoxic condition was less pronounced (Fig. 6A). On the other hand, combined treatment with 1 μM Gö6976 and 20 μM LY294002 enhanced the sensitivity of the cells to gemcitabine only under the normoglycemic/normoxic condition (Fig. 6B). In order to confirm if the effect of UCN-01 was due to inhibition of Chk1 activation or inhibition of some other target, the effect of the RNAi on Chk1 activation was examined. Chk1 siRNA and 20 μM LY294002 enhanced the sensitivity of the cells to gemcitabine under the normoglycemic/normoxic condition; however, it had no any effect under the hypoglycemic/hypoxic condition.

Discussion

As clearly shown in the present work, hypoxia and hypoglycemia had a large impact on the cellular sensitivity to anticancer drugs in different cancer cell lines. In most cases, the mechanism underlying the drug resistance is regarded as decreased cellular drug uptake. Multidrug resistance is one of major cellular mechanisms of drug resistance to a broad spectrum of anticancer drugs, and this phenotype is associated with an increased drug efflux from the cells caused by overexpression of the ABC transporter. In the present work, hypoglycemic/hypoxic condition also induced multidrug resistance; however, our findings clearly indicated that there was no reduction of gemcitabine uptake and incorporation under the hypoglycemic/hypoxic condition. The S-phase population was similar under the normoglycemic/normoxic and hypoglycemic/hypoxic conditions, with accompanying S-phase prolongation. S-phase prolongation might be due to the depletion of *de novo* synthesis of nucleotides caused by

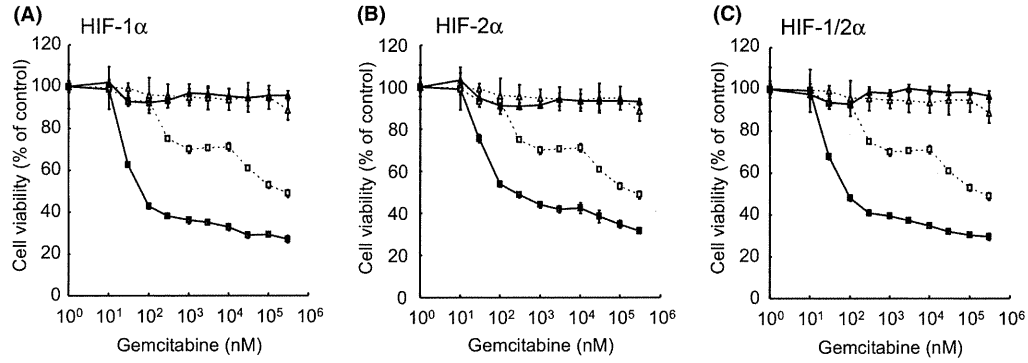

Fig. 5. Effect of combined inhibition of Chk1 and HIF signaling on the sensitivity of the cells to gemcitabine. Cells were treated with gemcitabine in the presence or absence of 1 μM UCN-01 plus RNAi for (A) HIF-1α, (B) HIF-2α or (C) HIF-1/2α under (■ or □) normoglycemic/normoxic condition or (▲ or △) normoglycemic/hypoxic condition.

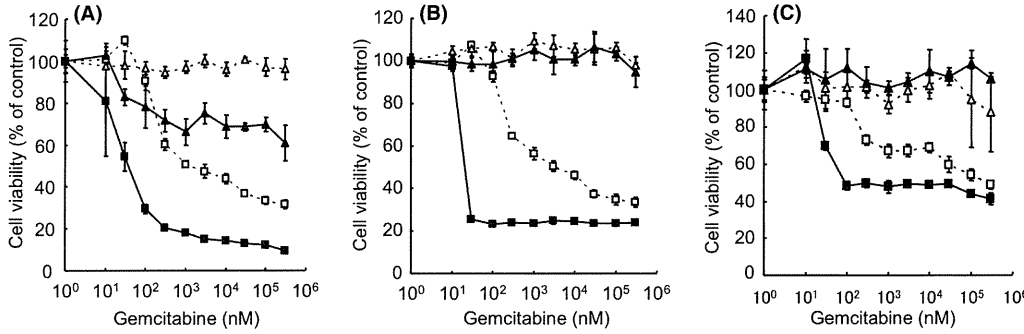

Fig. 6. Effect of combined inhibition of Chk1 and PI3K on the sensitivity of the cells to gemcitabine. Cells were treated with gemcitabine in the presence or absence of 1 μM (A) UCN-01, (B) 1 μM Gö6976 or (C) RNAi for Chk1, and 20 μM LY294002 under (■ or □) normoglycemic/normoxic condition or (▲ or △) hypoglycemic/hypoxic condition.

insufficiency of the pentose phosphate shunt supply. Nevertheless, it was not involved in DNA incorporation of gemcitabine under the hypoglycemic/hypoxic condition. Following its incorporation into DNA, gemcitabine blocks the extension of DNA and stall replication forks, leading to DNA damage. The DNA damage is recognized by sensor molecules that recruit and phosphorylate H2AX protein in the damaged DNA region.[44] Sensor molecules also phosphorylate checkpoint kinase causing its activation and arresting the cell cycle in the S phase.[45] The present study showed that phosphorylation of H2AX, Chk1 and Chk2 were induced by gemcitabine equally under the normoglycemic/normoxic and hypoglycemic/hypoxic conditions, leading to S-phase arrest. During checkpoint kinase activation and cell cycle arrest, phosphorylation of H2AX is known to be recruited by other DNA repair proteins, such as Mre11/Rad50/Nbs1, in the DNA damage region, resulting in activation of the DNA repair pathway.[46,47] Chronic hypoxia has been reported to suppress DNA repair protein activity.[48,49] The increased DNA incorporation of gemcitabine under the hypoglycemic/hypoxic condition may be caused by suppression of the DNA repair pathway.

Modulation of the cellular responses to DNA-damaging agents by checkpoint abrogators or inhibitors of cell survival signaling is an active area of research, since it has been believed that the interference of these signalings may enhance the therapeutic efficacy of anticancer drugs.[50] The S-phase checkpoint consists of a hierarchal regulatory cascade initiated by the activation of Chk1. In the present work, Chk1 inhibitors and Chk1 siRNA enhanced the cytotoxicity of gemcitabine under the normoglycemic/normoxic condition, consistent with other reports.[51–54] However, the abrogation of Chk1 activation did not affect the sensitivity of the cells to gemcitabine under the hypoglycemic/hypoxic condition. Tumor hypoxia has been well-studied, and previous reports have proposed that HIF-1α plays a critical role in determining cell survival and death,[40,41] while knockdown of HIF1α or HIF2α using siRNA did not affect the sensitivity of the cells to gemcitabine under the hypoxic condition in the present study. The PI3K/Akt pathway is well-known for its anti-apoptotic and cell survival activity under various conditions, including hypoxia and hypoglycemia,[55–57] but our results showed that the PI3K inhibitor LY294002 sensitized the cells to gemcitabine only under the normoglycemic/normoxic condition. We examined combined inhibition of Chk1 and of the cell survival pathways-sensitized cells to gemcitabine under the hypoglycemic/hypoxic condition. In the present work, the combination of UCN-01 and LY294002 partly abrogated the hypoglycemic/hypoxia-induced drug resistance, whereas the combination of Gö6976 or Chk1 siRNA with LY294002 had no such effect. These observations suggest that UCN-01 had a different target from Gö6976 in the mechanism of sensitizing the cells to gemcitabine under the hypoglycemic/hypoxic condition. UCN-01 has been reported to induce apoptosis in S-phase-arrested cells, not through Chk1 inhibition, although the precise mechanisms remain poorly understood.[58] We attempted to identify the kinase signaling responsible for the hypoglycemic/hypoxia-induced drug resistance in the targets of UCN-01; however, we did not obtain any clear results. PI3K and Akt are strongly expressed in some cancers, and have been found to be associated with a poor prognosis and increased tumor aggressiveness.[59,60] We previously reported that Akt

doi: 10.1111/j.1349-7006.2011.01880.x

expression was closely associated with cellular tolerance for nutrient deprivation.[61] The present work showed that Akt phosphorylation had a significant impact on the sensitivity of the PANC-1 cells to anticancer drugs.

In this study, we showed that hypoglycemic/hypoxic condition induced multidrug resistance. Combined kinase activations were involved in the hypoglycemic/hypoxia-induced drug resistance. Although the mechanism of cell death caused by gemcitabine is still unclear, the combined strategies described in the text might enhance the cytotoxicity of gemcitabine in clinical practice.

Acknowledgments

This work was supported by a Grant for the Third-Term Comprehensive 10-year Strategy for Cancer Control and 5-year Strategy for the Creation of Innovative Pharmaceuticals and Medical Devices from the Ministry of Health, Labour and Welfare, Japan.

Disclosure statement

No conflict of interest.

References

1 Jain RK. Molecular regulation of vessel maturation. *Nat Med* 2003; **9**: 685–93.
2 Thomlinson RH, Gray LH. The histological structure of some human lung cancers and the possible implications for radiotherapy. *Br J Cancer* 1955; **9**: 539–49.
3 Less JR, Skalak TC, Sevick EM, Jain RK. Microvascular architecture in a mammary carcinoma: branching patterns and vessel dimensions. *Cancer Res* 1991; **51**: 265–73.
4 Brown JM, Giaccia AJ. The unique physiology of solid tumors: opportunities (and problems) for cancer therapy. *Cancer Res* 1998; **58**: 1408–16.
5 Hockel M, Vaupel P. Tumor hypoxia: definitions and current clinical, biologic, and molecular aspects. *J Natl Cancer Inst* 2001; **93**: 266–76.
6 Harris AL. Hypoxia – a key regulatory factor in tumour growth. *Nat Rev Cancer* 2002; **2**: 38–47.
7 Bertout JA, Patel SA, Simon MC. The impact of O_2 availability on human cancer. *Nat Rev Cancer* 2008; **8**: 967–75.
8 Gatenby RA, Gillies RJ. Why do cancers have high aerobic glycolysis? *Nat Rev Cancer* 2004; **4**: 891–9.
9 Gillies RJ, Raghunand N, Karczmar GS, Bhujwalla ZM. MRI of the tumor microenvironment. *J Magn Reson Imaging* 2002; **16**: 430–50.
10 Semenza GL. HIF-1, O(2), and the 3 PHDs: how animal cells signal hypoxia to the nucleus. *Cell* 2001; **107**: 1–3.
11 Price BD, Calderwood SK. Gadd45 and Gadd153 messenger RNA levels are increased during hypoxia and after exposure of cells to agents which elevate the levels of the glucose-regulated proteins. *Cancer Res* 1992; **52**: 3814–7.
12 Wang GL, Semenza GL. Characterization of hypoxia-inducible factor 1 and regulation of DNA binding activity by hypoxia. *J Biol Chem* 1993; **268**: 21513–8.
13 Ryan HE, Lo J, Johnson RS. HIF-1 alpha is required for solid tumor formation and embryonic vascularization. *The EMBO J* 1998; **17**: 3005–15.
14 Maxwell PH, Dachs GU, Gleadle JM *et al.* Hypoxia-inducible factor-1 modulates gene expression in solid tumors and influences both angiogenesis and tumor growth. *Proc Natl Acad Sci U S A* 1997; **94**: 8104–9.
15 Carmeliet P, Dor Y, Herbert JM *et al.* Role of HIF-1alpha in hypoxia-mediated apoptosis, cell proliferation and tumour angiogenesis. *Nature* 1998; **394**: 485–90.
16 Warburg O. On the origin of cancer cells. *Science* 1956; **123**: 309–14.
17 Vander Heiden MG, Cantley LC, Thompson CB. Understanding the Warburg effect: the metabolic requirements of cell proliferation. *Science* 2009; **324**: 1029–33.
18 Chen Z, Lu W, Garcia-Prieto C, Huang P. The Warburg effect and its cancer therapeutic implications. *J Bioenerg Biomembr* 2007; **39**: 267–74.
19 Kondoh H. Cellular life span and the Warburg effect. *Exp Cell Res* 2008; **314**: 1923–8.
20 Hirayama A, Kami K, Sugimoto M *et al.* Quantitative metabolome profiling of colon and stomach cancer microenvironment by capillary electrophoresis time-of-flight mass spectrometry. *Cancer Res* 2009; **69**: 4918–25.
21 Savage P, Stebbing J, Bower M, Crook T. Why does cytotoxic chemotherapy cure only some cancers? *Nat Clin Pract Oncol* 2009; **6**: 43–52.
22 Minchinton AI, Tannock IF. Drug penetration in solid tumours. *Nat Rev Cancer* 2006; **6**: 583–92.
23 Tsuruo T, Naito M, Tomida A *et al.* Molecular targeting therapy of cancer: drug resistance, apoptosis and survival signal. *Cancer Sci* 2003; **94**: 15–21.
24 Sugimoto Y, Tsuruo T. DNA-mediated transfer and cloning of a human multidrug-resistant gene of adriamycin-resistant myelogenous leukemia K562. *Cancer Res* 1987; **47**: 2620–5.
25 Hamada H, Tsuruo T. Functional role for the 170- to 180-kDa glycoprotein specific to drug-resistant tumor cells as revealed by monoclonal antibodies. *Proc Natl Acad Sci U S A* 1986; **83**: 7785–9.
26 Ho WJ, Pham EA, Kim JW *et al.* Incorporation of multicellular spheroids into 3-D polymeric scaffolds provides an improved tumor model for screening anticancer drugs. *Cancer Sci* 2010; **101**: 2637–43.
27 Liao Q, Hu Y, Zhao YP, Zhou T, Zhang Q. Assessment of pancreatic carcinoma cell chemosensitivity using a three-dimensional culture system. *Chin Med J (Engl)* 2010; **123**: 1871–7.
28 Lu J, Kunimoto S, Yamazaki Y, Kaminishi M, Esumi H. Kigamicin D, a novel anticancer agent based on a new anti-austerity strategy targeting cancer cells' tolerance to nutrient starvation. *Cancer Sci* 2004; **95**: 547–52.
29 Awale S, Lu J, Kalauni SK *et al.* Identification of arctigenin as an antitumor agent having the ability to eliminate the tolerance of cancer cells to nutrient starvation. *Cancer Res* 2006; **66**: 1751–7.
30 Wong SJ, Myette MS, Wereley JP, Chitambar CR. Increased sensitivity of hydroxyurea-resistant leukemic cells to gemcitabine. *Clin Cancer Res* 1999; **5**: 439–43.
31 Imamura T, Kanai F, Kawakami T *et al.* Proteomic analysis of the TGF-beta signaling pathway in pancreatic carcinoma cells using stable RNA interference to silence Smad4 expression. *Biochem Biophys Res Commun* 2004; **318**: 289–96.
32 Sampath D, Rao VA, Plunkett W. Mechanisms of apoptosis induction by nucleoside analogs. *Oncogene* 2003; **22**: 9063–74.
33 Ewald B, Sampath D, Plunkett W. Nucleoside analogs: molecular mechanisms signaling cell death. *Oncogene* 2008; **27**: 6522–37.
34 Zhang YW, Hunter T, Abraham RT. Turning the replication checkpoint on and off. *Cell Cycle* 2006; **5**: 125–8.
35 Sampath D, Shi Z, Plunkett W. Inhibition of cyclin-dependent kinase 2 by the Chk1-Cdc25A pathway during the S-phase checkpoint activated by fludarabine: dysregulation by 7-hydroxystaurosporine. *Mol Pharmacol* 2002; **62**: 680–8.
36 Facchinetti MM, De Siervi A, Toskos D, Senderowicz AM. UCN-01-induced cell cycle arrest requires the transcriptional induction of p21(waf1/cip1) by activation of mitogen-activated protein/extracellular signal-regulated kinase kinase/extracellular signal-regulated kinase pathway. *Cancer Res* 2004; **64**: 3629–37.
37 Monks A, Harris ED, Vaigro-Wolff A, Hose CD, Connelly JW, Sausville EA. UCN-01 enhances the in vitro toxicity of clinical agents in human tumor cell lines. *Invest New Drugs* 2000; **18**: 95–107.
38 Ewald B, Sampath D, Plunkett W. H2AX phosphorylation marks gemcitabine-induced stalled replication forks and their collapse upon S-phase checkpoint abrogation. *Mol Cancer Ther* 2007; **6**: 1239–48.
39 Kohn EA, Yoo CJ, Eastman A. The protein kinase C inhibitor Go6976 is a potent inhibitor of DNA damage-induced S and G2 cell cycle checkpoints. *Cancer Res* 2003; **63**: 31–5.
40 Semenza GL. Targeting HIF-1 for cancer therapy. *Nat Rev Cancer* 2003; **3**: 721–32.
41 Koukourakis MI, Giatromanolaki A, Sivridis E *et al.* Hypoxia-inducible factor (HIF1A and HIF2A), angiogenesis, and chemoradiotherapy outcome of squamous cell head-and-neck cancer. *Int J Radiat Oncol Biol Phys* 2002; **53**: 1192–202.
42 Chen EY, Mazure NM, Cooper JA, Giaccia AJ. Hypoxia activates a platelet-derived growth factor receptor/phosphatidylinositol 3-kinase/Akt pathway that results in glycogen synthase kinase-3 inactivation. *Cancer Res* 2001; **61**: 2429–33.
43 Esumi H, Izuishi K, Kato K *et al.* Hypoxia and nitric oxide treatment confer tolerance to glucose starvation in a 5′-AMP-activated protein kinase-dependent manner. *J Biol Chem* 2002; **277**: 32791–8.
44 Bonner WM, Redon CE, Dickey JS *et al.* GammaH2AX and cancer. *Nat Rev Cancer* 2008; **8**: 957–67.
45 Tse AN, Carvajal R, Schwartz GK. Targeting checkpoint kinase 1 in cancer therapeutics. *Clin Cancer Res* 2007; **13**: 1955–60.
46 Ewald B, Sampath D, Plunkett W. ATM and the Mre11-Rad50-Nbs1 complex respond to nucleoside analogue-induced stalled replication forks and contribute to drug resistance. *Cancer Res* 2008; **68**: 7947–55.
47 Parsels LA, Morgan MA, Tanska DM *et al.* Gemcitabine sensitization by checkpoint kinase 1 inhibition correlates with inhibition of a Rad51 DNA damage response in pancreatic cancer cells. *Mol Cancer Ther* 2009; **8**: 45–54.